

A Lagrangean Heuristic Approach for the Simultaneous Cyclic Scheduling and Optimal Control of Multi-Grade Polymerization Reactors.

Sebastian Terrazas-Moreno, Antonio Flores-Tlacuahuac*

Departamento de Ingeniería y Ciencias Químicas, Universidad Iberoamericana
Prolongación Paseo de la Reforma 880, México D.F., 01210, México

Ignacio E. Grossmann

Department of Chemical Engineering, Carnegie-Mellon University
5000 Forbes Av., Pittsburgh 15213, PA

April 8, 2006

*Author to whom correspondence should be addressed. E-mail: antonio.flores@uia.mx, phone/fax: +52(55)59504074, <http://200.13.98.241/~antonio>

Abstract

In this work we apply a decomposition technique to address the simultaneous scheduling and optimal control problem of multi-grade polymerization reactors. The simultaneous scheduling and control (SSC) problem is reformulated using Lagrangean Decomposition as presented by Guignard and Kim¹. The resulting model is decomposed into scheduling and control subproblems, and solved using a heuristic approach used before by Van den Heever et.al.² in a different kind of problem. The methodology is tested using a Methyl Methacrylate (MMA) polymerization system, and the High Impact Polystyrene (HIPS) polymerization system, with one continuous stirred-tank reactor (CSTR), and with a complete HIPS polymerization plant composed of a train of seven CSTRs. In these case studies, different polymer grades are produced using the same equipment in a cyclic schedule. The results of the heuristic decomposition technique are compared against those obtained by solving the problem without decomposition, whenever both solutions were available. The presence of a duality gap for the decomposed solution is observed, as expected, when integer variables and other nonconvexities are present. Computational times in the first two examples were lower for the decomposition heuristic than for the direct solution in full space, and the optimal solutions found were slightly better. The example related to the full scale HIPS plant was only solvable using the decomposition heuristic.

1 Introduction

The simultaneous scheduling and control (SSC) problem involves determining the best sequencing of products for a manufacturing operation, while at the same time determining the optimal dynamic trajectories during product transitions. The simultaneous approach has shown to result in improved operation of certain chemical engineering systems compared to the traditional sequential approach^{3,4}. The sequential approach involves the determination of the production schedule and the optimal product transitions in two different steps. The SSC problem in polymerization systems has been addressed in a number of ways^{4,5,6,7,8,9,10}. Some works compare different product transitions for a polymerization CSTR^{5,6}. In these works robust control theory is employed to propose screening tools and heuristics for determining favorable transitions, and a preferred schedule is proposed based on those tools. Prata et.al.⁷ propose a simultaneous scheduling and control formulation in which the dynamic optimization part is solved using multiple shooting techniques. This formulation was tested using a continuous polymerization reaction system under different demand patterns (with and without due dates). Nystrom et. al.^{8,9} propose a solution methodology for the SSC problem in which the original MIDO formulation is decoupled into a master scheduling problem and a primal control problem. The two problems are solved separately in an iterative manner, while information regarding key high level parameters is exchanged between them. The key high level parameters exchanged include transition and production times obtained from the primal problem, and are included in the solution of the master problem. This methodology completely decouples the sequencing and the control problem. The solution to be proposed in this paper is different from the last two references discussed^{8,9} since the two subproblems in the present work, share a common set of dualized constraints. Therefore, the SSC problem is decomposed rather than decoupled. In other works^{4,10}, assuming cyclic schedules, the SSC problem in multiproduct CSTRs turned out to be a MIDO problem which was solved using the Simultaneous Dynamic Optimization (SDO) approach¹¹.

The objective of this paper is to solve the Simultaneous Scheduling and Control (SSC) problem based on our previous formulation⁴ by exploiting its decomposable nature through a Lagrangean Decomposition technique¹. The SSC model reformulated using the decomposition technique is solved using a heuristic iterative procedure known to be useful for MINLP problems. In this procedure a set of upper bounds for the maximization problem is obtained through the rigorous solution of the decomposed model, while lower bounds are obtained by solving an NLP in which the binary variables are fixed using heuristics. Van den Heever et.al.² found that this technique can greatly reduce the time spent solving large MINLPs in the area of oil field planning. The same work also shows that if the problem size is large enough the decomposition heuristic allows the solution of otherwise unsolvable problems.

The idea of applying decomposition techniques to large scale scheduling problems has been presented before. A good example is the work by de Matta¹², where a Lagrangean decomposition is used to solve a single line multiproduct scheduling problem. This work is similar to ours in that it minimizes total inventory and changeover costs over a certain number of production periods. However, de Matta does not consider transition dynamics, changeover time is assumed to be negligible, and changeover cost is not dependent on product sequence. Another example of the use of decomposition techniques for scheduling problems is presented by Wu et.al.¹³. In this work a number of different decomposition approaches are used in a reaction-separation sequence, represented by a state task network. One of these approaches is the Lagrangean decomposition, which once again is coupled with a heuristic technique in order to generate a sequence of upper and lower bounds. This work does not take into consideration the dynamics of transitions, which is the fundamental feature of our SSC formulation. As a follow up to that work¹³ Wu et.al.¹⁴ worked on an improved approach for updating the Lagrangean multipliers, and apply their findings to a scheduling problem. Their formulation still does not include process dynamics, but it does take care of the disadvantages of the most common methods for updating the Lagrangean multipliers, although it carries added complexity.

In this paper Lagrangean decomposition of the SSC problem in polymerization reactors is proposed. An analysis is made on the size of the resulting subproblems, the computational effort and the optimal solution. The performance of this technique is compared against the direct solution obtained in the full space, whenever both were obtainable. In the remainder of this paper the term “direct solution” refers to the solution obtained in the full solution space, without decomposing the SSC problem.

2 Problem definition

Previously, we have proposed a simultaneous scheduling and control (SSC) formulation for polymerization reactors⁴. In the present paper the same problem definition for the SSC problem will be used. The objective of the SSC problem is determining the optimal production campaign in a cyclic polymerization operation, where the production of different polymer grades is carried out using the same equipment. Different polymer grades are obtained from the same raw material using different process conditions, which result in different end product characteristics. The optimal cycle is described by the following decision variables: (1) grade manufacturing sequence, (2) variables involved in dynamic transitions, (3) cycle duration, (4) amounts of grades produced. Certain assumptions are made in order to obtain the optimal solution: (a) demand, inventory costs and raw material costs are deterministic parameters, (b) all polymer produced is sold; there is no upper bound on production, (c) all grades are produced only once during the production cycle, (d) once a grade has been produced it is stored and depleted until the end of the cycle, (e) profit is defined as product sales minus inventory holding costs minus transition costs divided by total cycle time (hourly profit).

The scheduling and the control problems in the SSC formulation share a limited number of variables. In the formulation used in this paper such variables are binary sequencing variables, transitions duration, and cycle duration. The Lagrangean Decomposition technique exploits this characteristic and reformulates the SSC problem to obtain two

separable subproblems. This paper is concerned with the solution of the decomposed SSC problem in polymerization reactors, and the comparison of this solution against that obtained by a direct solution.

3 Scheduling and Control MIDO Formulation

For convenience to the reader, we present the model in⁴ in concise form. For a detailed description of the model see⁴. The manufacturing operation relevant to this work is carried out in production cycles. The cycle time is divided into a series of slots. Within each slot two operations are carried out: (a) the production period during which a given product is manufactured around steady-state conditions, and (b) the transition period during which dynamic transitions between two products take place. It is assumed that only one product can be produced in a slot and that each product is produced only once within each production wheel. Also, once a production wheel is completed, new identical cycles are executed indefinitely. The notation is listed in detail in the appendix.

- **Objective function.**

$$\max \left\{ \begin{aligned} & \sum_{i=1}^{N_p} \frac{C_i^p W_i}{T_c} - \sum_{i=1}^{N_p} \frac{C_i^s (G_i - W_i/T_c) \Theta_i}{2} \\ & - \left[\sum_{k=1}^{N_s} \sum_{f=1}^{N_{fe}} h_{fk} \theta_k^t Q_{max}^m \sum_{c=1}^{N_{cp}} u_{fck}^m \gamma_c \right] \frac{C^r}{T_c} \\ & - \left[\sum_{k=1}^{N_s} \sum_{f=1}^{N_{fe}} h_{fk} \theta_k^t Q_{max}^I \sum_{c=1}^{N_{cp}} u_{fck}^I \gamma_c \right] \frac{C^I}{T_c} \end{aligned} \right\} \quad (1)$$

The total process profit is given by the income of the manufactured products minus the sum of the inventory costs and the product transition costs. All terms are divided by the cyclic time (T_c) so that the objective function value corresponds to the cyclic hourly profit.

In order to clarify the SSC MIDO problem formulation, the constraints have been divided into two parts: (1) scheduling part, and (2) dynamic optimization part.

1. Scheduling.

a) Product assignment

$$\sum_{k=1}^{N_s} y_{ik} = 1, \forall i \quad (2a)$$

$$\sum_{i=1}^{N_p} y_{ik} = 1, \forall k \quad (2b)$$

where

y_{ik} Binary variable to denote if product i is produced at slot k

b) Amounts manufactured

$$W_i \geq D_i T_c, \forall i \quad (3a)$$

$$W_i = G_i \Theta_i, \forall i \quad (3b)$$

$$G_i = F_i^o C_{m0} \frac{MW_{monomer}}{1000}, \forall i \quad (3c)$$

c) Processing times

$$\theta_{ik} \leq \theta^{max} y_{ik}, \forall i, k \quad (4a)$$

$$\Theta_i = \sum_{k=1}^{N_s} \theta_{ik}, \forall i \quad (4b)$$

$$p_k = \sum_{i=1}^{N_p} \theta_{ik}, \forall k \quad (4c)$$

e) Timing relations

$$t_k^e = t_k^s + p_k + \theta_k^t, \forall k \quad (5a)$$

$$t_k^s = t_{k-1}^e, \forall k \neq 1 \quad (5b)$$

$$t_k^e \leq T_c, \forall k \quad (5c)$$

$$t_{fck} = (f-1) \frac{\theta_k^t}{N_{fe}} + \frac{\theta_k^t}{N_{fe}} \gamma_c, \forall f, c, k \quad (5d)$$

2. Dynamic Optimization.

To address the optimal control part, the simultaneous approach¹¹ for dynamic optimization problems was used in which the dynamic model representing the system behavior is discretized using the method of orthogonal collocation on finite elements^{15,16}. According to this procedure, a given slot k is divided into a number of finite elements. Within each finite element an adequate number of internal collocation points is selected. Using several finite elements is useful to represent dynamic profiles with non-smooth variations. Thus, the set of ordinary differential equations comprising the system model, is approximated at each collocation point leading to a set of nonlinear equations that must be satisfied.

a) Dynamic mathematical model discretization

$$x_{fck}^n = x_{o,fk}^n + \theta_k^t h_{fk} \sum_{l=1}^{N_{cp}} \Omega_{lc} \dot{x}_{flk}^n, \forall n, f, c, k \quad (6)$$

Also note that in the present formulation the length of all finite elements is the

same and computed as

$$h_{fk} = \frac{1}{N_{fe}} \quad (7)$$

b) Continuity constraint between finite elements

$$x_{o,fk}^n = x_{o,f-1,k}^n + \theta_k^t h_{f-1,k} \sum_{l=1}^{N_{cp}} \Omega_{l,N_{cp}} \dot{x}_{f-1,l,k}^n, \quad \forall n, f \geq 2, k \quad (8)$$

c) Model behavior at each collocation point

$$\dot{x}_{fck}^n = f^n(x_{fck}^1, \dots, x_{fck}^n, u_{fck}^1, \dots, u_{fck}^m), \quad \forall n, f, c, k \quad (9)$$

d) Initial and final controlled and manipulated variable values at each slot:

$$x_{in,k}^n = \sum_{i=1}^{N_p} x_{ss,i}^n y_{i,k}, \quad \forall n, k \quad (10)$$

$$\bar{x}_k^n = \sum_{i=1}^{N_p} x_{ss,i}^n y_{i,k+1}, \quad \forall n, k \neq N_s \quad (11)$$

$$\bar{x}_k^n = \sum_{i=1}^{N_p} x_{ss,i}^n y_{i,1}, \quad \forall n, k = N_s \quad (12)$$

$$u_{in,k}^m = \sum_{i=1}^{N_p} u_{ss,i}^m y_{i,k}, \quad \forall m, k \quad (13)$$

$$\bar{u}_k^m = \sum_{i=1}^{N_p} u_{ss,i}^m y_{i,k+1}, \quad \forall m, k \neq N_s - 1 \quad (14)$$

$$\bar{u}_k^m = \sum_{i=1}^{N_p} u_{ss,i}^m y_{i,1}, \quad \forall m, k = N_s \quad (15)$$

$$u_{1,1,k}^m = u_{in,k}^m, \quad \forall m, k \quad (16)$$

$$x_{o,1,k}^n = x_{in,k}^n, \quad \forall n, k \quad (17)$$

$$x_{tol,k}^n \geq x_{N_{fe},N_c,k}^n - \bar{x}_k^n, \quad \forall n, k \quad (18)$$

$$-x_{tol,k}^n \leq x_{N_{fe},N_c,k}^n - \bar{x}_k^n, \quad \forall n, k \quad (19)$$

e) Lower and upper bounds on the decision variables

$$x_{min}^n \leq x_{fck}^n \leq x_{max}^n, \forall n, f, c, k \quad (20a)$$

$$u_{min}^m \leq u_{fck}^m \leq u_{max}^m, \forall m, f, c, k \quad (20b)$$

f) Smooth transition constraints

$$u_{f,c,k}^m - u_{f,c-1,k}^m \leq u_{cont}^c, \forall m, k, c \neq 1 \quad (21)$$

$$u_{f,c,k}^m - u_{f,c-1,k}^m \geq -u_{cont}^c, \forall m, k, f, c \neq 1 \quad (22)$$

$$u_{f,1,k}^m - u_{f-1,Nfe,k}^m \leq u_{cont}^f, \forall m, k, f \neq 1 \quad (23)$$

$$u_{f,1,k}^m - u_{f-1,Nfe,k}^m \geq -u_{cont}^f, \forall m, k, f \neq 1 \quad (24)$$

$$u_{1,1,k}^m - u_{in,k}^m \leq u_{cont}^f, \forall k \quad (25)$$

$$u_{1,1,k}^m - u_{in,k}^m \geq -u_{cont}^f, \forall k \quad (26)$$

$$\dot{x}_{Nfe,Ncp,k}^n \geq -\dot{x}_{tol,k}, \forall n, k \quad (27)$$

$$\dot{x}_{Nfe,Ncp,k}^n \leq \dot{x}_{tol,k}, \forall n, k \quad (28)$$

Equations 21- 26 force the change between adjacent collocation points and finite elements to be within a certain acceptable range. Equations 27 and 28 are used to make sure that at the end of the dynamic transition the system is at, or very close to, steady state conditions.

4 Outline of the Solution Methodology

The nature of the problem at hand suggests the use of a decomposition technique in which the dynamic optimization problem and the scheduling problem are solved separately. The Lagrangean Decomposition technique¹ is the basis of the solution methodology presented

in this paper. The scheduling and control formulation share the binary variables associated with a production schedule: (1) the variables of transitions durations, and (2) the variable of cycle duration. These variables are substituted by equivalent copies in either the scheduling or the control problem, and a new set of constraints makes the copies equal to the original variables. This new set of constraints is dualized by adding them to the objective function using Lagrange multipliers¹⁷. This modified SSC formulation is separable into a scheduling subproblem and a control problem where the sum of the objective functions of the two subproblems (see later equations 31 and 32) represents an upper bound to the objective function of the SSC original problem. Van den Heever et.al.² propose a heuristic in which the binary variables in the original formulation are fixed so that a lower bound is obtained by solving the resulting NLP. In this paper the binary variables obtained in the scheduling subproblem are fixed in the original SSC formulation to obtain an NLP that yields a lower bound in each iteration of the heuristic decomposition algorithm. Once an upper bound and a lower bound are obtained one iteration is completed, after which the lagrangian multipliers are updated. This heuristic algorithm stops once the upper and lower bound converge within a defined tolerance or once the maximum number of iterations is exceeded. Since the algorithm is heuristic, the maximum number of iterations can be determined using different criteria. Generally this number will be set so that it stops when the algorithm is not making any significant progress, but it can also be determined by the point in which bounds begin to degrade or subproblems become infeasible. In MINLP problems a duality gap may exist between the optimal solution of the decomposed problem and the optimal solution to the original problem¹⁸. If this is the case, then the two bounds will not converge and the algorithm will reach the maximum number of iterations. If the maximum number of iterations is exceeded, then the best lower bound is reported as the solution. A formal mathematical description of the decomposition technique follows.

4.1 Lagrangean Decomposition

Guignard and Kim¹ present a Lagrangean Decomposition technique in which certain variables are duplicated and set equal by new constraints. These new constraints are then relaxed through Lagrangean Relaxation^{17,19}, yielding a decomposable model over two or more subsets of constraints. Consider the following mathematical programming problem:

$$(P) \quad \max \{fx \mid Ax \leq b, Cx \leq d, x \in X\}$$

which is equivalent to:

$$(P') \quad \max \{fx \mid Ay \leq b, Cx \leq d, x \in X, y = x, y \in Y\}$$

A Lagrangean relaxation is obtained for P' by dualizing the constraint $y = x$. This procedure yields a decomposable problem, thus the name “Lagrangean Decomposition”:

$$\begin{aligned} (LDu) \\ \max \{fx + u(y - x) \mid Cx \leq d, x \in X, \\ Ay \leq b, y \in Y\} \\ = \max \{(f - u)x \mid Cx \leq d, x \in X\} \\ + \max \{uy \mid Ay \leq b, y \in Y\} \end{aligned}$$

If the constraints are convex then LDu is an upper bound for P for any given u ¹⁷. Then if all of the constraints are convex and all of the variables are continuous, the tightest upper bound of LDu is equal to the optimal solution of P :

$$P = \min_u LDu$$

In the presence of integer variables and other nonconvexities a duality gap may exist¹⁸.

Since this is the case of the current formulation, the search for an optimum will be performed using an heuristic approach² that generates upper bounds by solving a problem of the type LDu and lower bounds by using a heuristic technique to produce feasible solutions to the original problem P . The multipliers used to solve the subproblems are updated iteratively using the Fisher formula that has proven to work well in practice²⁰:

$$u^{k+1} = u^k + t^k(y^k - x^k)$$

and

$$t^{k+1} = \frac{\alpha_k(LD(u^k) - P^*)}{\|y^k - x^k\|^2}$$

where t^k is a scalar step size and α is a scalar usually set between 0 and 2 and then decreased when LDU fails to improve in a fixed number of iterations. This method for updating the multipliers is known as the subgradient method.

4.2 Lagrangean decomposition for integer programming.

Michelon and Maculan²¹ present the extension of Lagrangean Decomposition for integer nonlinear programming with linear constraints. Using again the example of problem (P), but in the context of integer programming, we have the following:

$$(P) \quad \max \{fx | Ax \leq b, Cx \leq d, x \in X\}$$

Where X is a set for which the integrality constraints are defined, e.g. $X = \{0, 1\}$.

The feasible domain of (P) remains unchanged²¹ if we add the constrains:

$$y = x, \quad Ay \leq b, \quad Cx \leq d \quad \text{and} \quad y \in CO(X)$$

where $CO(X)$ represents the Convex Hull of set X

A Lagrangean relaxation is obtained for (P) by dualizing the constraint $y = x$. The

same procedure described under the Lagrangean Decomposition section of this paper can be followed afterwards.

The important fact to take notice of is that the copy (y) of the original binary variable (x) is continuous, since the domain of the new variable is the convex hull of X , denoted as $CO(X)$. As mentioned above the set $X = \{0, 1\}$, and its convex hull includes all real numbers between 0 and 1. This fact is of the utmost importance for the development of the decomposition in this paper, since it allows the treatment of binary variables in the scheduling subproblem, while their continuous copies are used in the nonlinear control subproblem.

5 Scheduling and Control MIDO Reformulation

The problem reformulation consists of four steps.

1. Duplicate key variables.

$$z_{ik} = y_{ik}, \forall i, k, y \in B, z \in CO(B) \quad (29a)$$

$$\phi_k^t = \theta_k^t, \forall k \quad (29b)$$

$$Dc = Tc \quad (29c)$$

where

B Set of binary values $\{0,1\}$

$CO(B)$ Convex Hull of set B

Equations 29a to 29c create copies of the sequencing variable, the transition duration variable and the cycle duration variable. It is important to notice that while y is binary variable ($y \in B$), z can take any value between 0 and 1 ($z \in CO(B)$)²¹.

2. Assign one copy of each variable to the scheduling constraints and the other to the dynamic optimization constraints; add necessary extra constraints

- ϕ_k^t substitutes θ_k^t in equations 5a, 5d, 6, and 8.
- The following two equations are duplicates of 2a and 2b:

$$\sum_{k=1}^{N_s} z_{ik} = 1, \forall i \quad (30a)$$

$$\sum_{i=1}^{N_p} z_{ik} = 1, \forall k \quad (30b)$$

- Dc substitutes Tc in the transition terms of the objective function.

3. Equations 29a,29b, and 29c are eliminated and added to the objective function by means of a Lagrangian Relaxation¹⁷.

The objective function takes the following form:

$$\begin{aligned} \max \quad & \left\{ \sum_{i=1}^{N_p} \frac{C_i^p W_i}{T_c} - \sum_{i=1}^{N_p} \frac{C_i^s (G_i - W_i/T_c) \theta_i}{2} \right. \\ & - \left[\sum_{k=1}^{N_s} \sum_{f=1}^{N_{fe}} h_{fk} \theta_k^t Q_{max}^m \sum_{c=1}^{N_{cp}} u_{fck}^m \gamma_c \right] \frac{C^r}{D_c} \\ & - \left[\sum_{k=1}^{N_s} \sum_{f=1}^{N_{fe}} h_{fk} \theta_k^t Q_{max}^I \sum_{c=1}^{N_{cp}} u_{fck}^I \gamma_c \right] \frac{C^I}{D_c} \\ & \left. + \sum_{k=1}^{N_s} \sum_{i=1}^{N_p} [\mu_y (z_{ik} - y_{ik})] + \sum_{k=1}^{N_s} [\mu_\theta (\phi_k^t - \theta_k^t)] + \mu_{Tc} (Dc - Tc) \right\} \end{aligned}$$

$\mu_y, \mu_\theta, \mu_{Tc}$ are the lagrangean multipliers. These quantities are updated after every iteration of the heuristic Lagrangean decomposition algorithm.

4. The formulation is decomposed into a scheduling subproblem and a control subproblem.

- Scheduling Subproblem.

$$\max \left\{ \sum_{i=1}^{N_p} \frac{C_i^p W_i}{T_c} - \sum_{i=1}^{N_p} \frac{C_i^s (G_i - W_i/T_c) \theta_i}{2} + \sum_{k=1}^{N_s} \sum_{i=1}^{N_p} [\mu_y(-y_{ik})] + \sum_{k=1}^{N_s} [\mu_\theta(-\theta_k^t)] + \mu_{T_c}(-T_c) \right\} \quad (31)$$

s.t.

Equations. 2a to 5c

- Control Subproblem

$$\max \left\{ - \left[\sum_{k=1}^{N_s} \sum_{f=1}^{N_{fe}} h_{fck} \theta_k^t Q_{max}^I \sum_{c=1}^{N_{cp}} u_{fck}^I \gamma_c \right] \frac{C^I}{D_c} - \left[\sum_{k=1}^{N_s} \sum_{f=1}^{N_{fe}} h_{fck} \theta_k^t Q_{max}^m \sum_{c=1}^{N_{cp}} u_{fck}^m \gamma_c \right] \frac{C^m}{D_c} + \sum_{k=1}^{N_s} \sum_{i=1}^{N_p} [\mu_y(z_{ik})] + \sum_{k=1}^{N_s} [\mu_\theta(\phi_k^t)] + \mu_{T_c}(D_c) \right\} \quad (32)$$

s.t.

Equations. 5d to 28, 30a and 30b

with variable y_{ik} substituted for z_{ik}

and variable θ_k^t substituted for ϕ_k^t

6 Case Studies

In the following section three polymerization reaction examples are used to illustrate the usefulness of the decomposition technique. The solution obtained using the full space (direct solution) and the scheduling subproblem of the decomposed formulation are MINLPs solved using DICOPT. The control subproblem of the decomposed formulation and the problem used to generate heuristic lower bounds are NLPs solved using CONOPT3. All models are written in GAMS and solved using a 2.0 GHz machine.

6.1 MMA polymerization

Process Description

The MMA polymerization system used in this paper is that described by Silva-Beard et.al.²². The polymerization reactions take place in a CSTR. Table 1 shows the design and operating parameters of the reactor. The mathematical model that describes the bulk free-radical MMA polymerization using AIBN as the initiator is described below:

$$\frac{dC_m}{dt} = -(k_p + k_{fm})C_m P_0 + \frac{F(C_{min} - C_{in})}{V} \quad (33)$$

$$\frac{dC_I}{dt} = -k_I C_I + \frac{F C_{Iin}}{V} - F C_I \quad (34)$$

$$\frac{dT}{dt} = \frac{(-\Delta H)k_p C_m}{\rho C_p} P_0 - \frac{UA}{\rho C_p V} (T - T_j) + \frac{F(T_{in} - T)}{V} \quad (35)$$

$$\frac{dD_0}{dt} = (0.5K_{tc} + k_{td})P_0^2 + k_{fm}C_m P_0 - \frac{FD_0}{V} \quad (36)$$

$$\frac{dD_1}{dt} = M_m(k_p + k_{fm})C_m P_0 - \frac{FD_1}{V} \quad (37)$$

$$\frac{dT_j}{dt} = \frac{F_{cw}(T_{w0} - T_j)}{V_0} + \frac{UA}{\rho C_{pw} V_0} (T - T_j); \quad (38)$$

where

$$P_0 = \sqrt{\frac{2f^* C_I k_I}{k_{td} + k_{tc}}}$$

$$k_r = A_r e^{-E/RT}, r = p, fm, I, td, tc$$

Five different MMA grades are produced, where each grade corresponds to a different steady state. Table 2 shows the values of the main process variables that correspond to each steady state. Solutions using the full space and a using the decomposition heuristic are easily computed with little computational effort. This example is included so the decomposition approach is analyzed using a simple example, and the results are validated against the solution found in the full solution space.

Results

In this section the results of the iterative heuristic decomposition technique are presented and compared against those obtained by solving the SSC model in full space (direct solution). Our main interest is analyzing the performance of the decomposition technique in terms of the optimal profit and the computational effort. Table 3 contains values of the main decision variables for the solutions found with and without using the decomposition technique. The values of the sequencing binary variables used to initialize both cases corresponds to the sequence $A \rightarrow B \rightarrow C \rightarrow D \rightarrow E$. The initialization values of all other decision variables are also identical between the direct and decomposed formulations.

Figure 1 shows the evolution of the upper and lower bounds during the Lagrangean iterative procedure. A drastic improvement in upper bounding from the relaxed solution is observed. In fact a very tight upper bound is obtained in the iteration, and even slightly improved in subsequent iterations. The heuristic lower bound obtained by fixing the binary variables of the original problem to their corresponding values for the scheduling subproblem in the decomposed formulation reaches its maximum value after two iterations. At this point the gap between bounds is approximately 1.5%. In fact, the algorithm could be said to converge in two iterations with a tolerance of 2% for the gap between bounds. For this illustrative example the algorithm is continued after two iterations to show how the improvement stalls after that point.

It is important to say that the duplicated variables that allow the decomposition, namely,

cycle time, transition time, and sequencing variables, do not converge to the same values during the algorithm, even though the optimal value of the decomposition (upper bound) converges to the optimal of the original problem (lower bound). This has been reported in previous works,^{14,23} and it is due to the effect of using the subgradient method for updating the Lagrange multipliers. This is not a serious problem for the heuristic method used in this work, since the optimal value reported is always determined from the best lower bound. This bound is obtained by fixing binary variables, and keeping all of the original problem constraints. Therefore, the solution obtained represents a feasible solution to the original, non-decomposed problem. The value of the upper bound is used only to certain determined convergence of the algorithm.

Table 3 shows computational times and optimal solutions for the decomposed and direct approaches (including all six iterations). The CPU solution time for the decomposed formulation is 21 seconds lower than for the direct formulation, and the optimum found is better. The solution time required using both techniques is relatively low (128 and 106 CPUs) in this illustrative example, but still a 16% reduction in the solution time is achieved. Table 4 shows the size of the direct formulation and of each of the subproblems involved in the decomposed formulation. This table includes the SSC formulation with fixed binary variables, used for obtaining the heuristic lower bound. In this table the increase in number of variables used for the decomposed formulation is evident. However, in the decomposed formulation binary variables are only present in the scheduling subproblem, since the sequencing variables for the control problem are continuous as shown in equation 29a. Therefore, in the decomposition technique the complicating integer variables are confined to a much smaller problem. From Table 4 one can see that the largest portion of solution time for the decomposition algorithm is spent solving the NLP that provides the lower bounds.

Comparison of optimal solutions.

The decomposition technique finds a better local optimum than the one found using the full solution space. Notice how the direct formulation optimum corresponds to the initial sequence provided to the solver. On the other hand, the decomposition results show a very different sequence. The iterative nature of the heuristic decomposition technique, where Lagrange multipliers are updated in every iteration, allows for a different local search every time. The profit of 83.6 \$/hr is still a local optimum for one set of values for the Lagrangian Multipliers.

Reference⁴ includes an extensive analysis of the behavior of different decision variables for the isothermal version of the MMA model presented in this work. The findings in⁴ can be applied to the comparison between the optimal profit for the direct approach and the decomposed approach. Raw material, inventory costs and product prices are the same as those used in⁴. Tables 5 and 6 show the values for the main decision variables for the direct and decomposed solution. Both solution share one important characteristic. Even though there is no upper bound on sales (all polymer produced is sold), all grades are produced exactly to meet demand; not even grade E, which is the most profitable, is produced more than it is demanded. This means that every extra hour that the cycle is extended the inventory costs incurred are greater than the profit generated by the extra production. In this scenario the cycle productivity, and the minimization of the time spent in grade transitions becomes very important.

Figures 4 and 5 show the dynamic transitions for the direct and decomposed solutions. The heuristic decomposition algorithm results in an optimal cycle characterized by faster transitions and a shorter, more productive cycle. Figures 4 and 5 show that the longest transition for the direct solution takes almost seven hours, while the longest transition for the decomposed approach takes less than four. For the decomposed solution the optimizer chooses transitions between non sequential grades (A to C, C to E, etc.). This avoids the need for a long transition at the end of the cycle. On the other hand the direct solution

chooses transitions between sequential grades (A to B, B to C, etc.) but is forced to make a very long transition (E to A) at the end of the cycle. The optimal trajectories for the decomposed approach show that for a couple of grade transitions the manipulated variable, namely, the initiator flow rate, is completely shut down for a while. This helps in making the transitions cheaper since less initiator is wasted in off-spec material.

6.2 HIPS polymerization reactor

Process Description

A second example is included with the goal of exploring the performance of the proposed approach in presence of a stronger nonlinear behavior and a larger problem. For that purpose the HIPS polymerization system²⁴ is employed. The polymerization is carried out in a CSTR. Table 7 shows the design and operating parameters of the reactor. The dynamic model of a CSTR where the non-isothermal high impact polymerization of styrene takes place is given as follows:

- Initiator concentration.

$$\frac{dC_i}{dt} = \frac{Q_i C_i^f - Q C_i}{V} - K_d C_i \quad (39)$$

- Monomer concentration.

$$\frac{dC_m}{dt} = \frac{Q}{V} (C_m^f - C_m) - K_p C_m (\mu_r^o + \mu_b^o) \quad (40)$$

- Butadiene concentration.

$$\frac{dC_b}{dt} = \frac{Q}{V} (C_b^f - C_b) - C_b (K_{i2} C_r + K_{fs} \mu_r^o + K_{fb} \mu_b^o) \quad (41)$$

- Radicals concentration.

$$\frac{dC_r}{dt} = -\frac{Q}{V} C_r + 2f^* K_d C_i - C_r (K_{i1} C_m + K_{i2} C_b) \quad (42)$$

- Branched radicals concentration.

$$\frac{dC_{br}}{dt} = -\frac{Q}{V}C_{br} + C_b(K_{i2}C_r + K_{fb}(\mu_r^o + \mu_b^o)) - C_{br}(K_{i3}C_m + K_t(\mu_r^o + \mu_b^o + C_{br})) \quad (43)$$

- Reactor temperature.

$$\frac{dT}{dt} = \frac{Q}{V}(T^f - T) + \frac{\Delta H_r K_p C_m (\mu_r^o + \mu_b^o)}{\rho_s C_{ps}} - \frac{UA(T - T_j)}{\rho_s C_{ps} V} \quad (44)$$

- Cooling jacket temperature.

$$\frac{dT_j}{dt} = \frac{Q_w}{V_c}(T_j^f - T_j) + \frac{UA(T - T_j)}{\rho_w C_{pw} V_c} \quad (45)$$

- Zeroth moment live polymer.

$$\frac{d\lambda_p^o}{dt} = -\frac{Q}{V}\lambda_p^o + \frac{K_t}{2}(\mu_r^o)^2 + (K_{fs}C_m + K_{fb}C_b)\mu_r^o \quad (46)$$

- First moment live polymer.

$$\frac{d\lambda_p^1}{dt} = -\frac{Q}{V}\lambda_p^1 + K_t\mu_r^1\mu_r^o + (K_{fs}C_m + K_{fb}C_b)\mu_r^1 \quad (47)$$

- Zeroth moment dead polymer.

$$\begin{aligned} \frac{d\mu_r^o}{dt} = & -\frac{Q}{V}\mu_r^o + 2K_{io}C_m^3 + K_{i1}C_rC_m + C_mK_{fs}(\mu_r^o + \mu_b^o) \\ & - (K_pC_m + K_t(\mu_r^o + \mu_b^o + C_{br})) + K_{fs}C_m + K_{fb}C_b)\mu_r^o + K_pC_m\mu_r^o \end{aligned} \quad (48)$$

- First moment dead polymer.

$$\begin{aligned} \frac{d\mu_r^1}{dt} = & -\frac{Q}{V}\mu_r^1 - (K_pC_m + K_t(\mu_r^o + \mu_b^o + C_{br})) + K_{fs}C_m + K_{fb}C_b)\mu_r^1 \\ & + K_pC_m(\mu_r^1 + \mu_r^o) \end{aligned} \quad (49)$$

- Zeroth moment butadiene.

$$\begin{aligned} \frac{d\mu_b^o}{dt} = & -\frac{Q}{V}\mu_b^o + K_{i3}C_{br}C_m - (K_pC_m + K_t(\mu_r^o + \mu_b^o + C_{br}) \\ & + K_{fs}C_m + K_{fb}C_b)\mu_b^o + K_pC_m\mu_b^o \end{aligned} \quad (50)$$

- Number molecular weight distribution.

$$M_n = \frac{\lambda_p^1 + \mu_r^1}{\lambda_p^o + \mu_r^o} \quad (51)$$

Five different HIPS grades are produced, where each grade corresponds to a different steady state. Table 8 shows the values of the main processes variables that correspond to each steady state.

Results

The behavior of the lower and upper bounding of the algorithm is presented in Figure 2, and the optimal solution and key decision variable values are presented in Table 9. From Figure 2, it is clear that there is a significant duality gap between upper and lower bounding. Using this same heuristic algorithm for an oilfield planning problem, Van den Heever et. al.² found differences of up 13.2% between upper and lower bounds which are similar in magnitude to the 8.6% present in the HIPS case study. From the same Figure, one can observe that the behavior of the upper bound is not always decreasing between sequential iterations. This behavior is normal when the Lagrange multipliers are updated using the subgradient method^{2,14,23}. Still there is an overall decrease of the upper bound as iterations increase up to the sixth iteration. Lower bounds do not follow a specific pattern, but this behavior is also expected since they are generated heuristically. After 6 iterations, the upper bound starts to deteriorate and the lower bounding problem becomes infeasible, so the algorithm is stopped. Two important points observed from the results in Table 9 are that the optimal value found by the decomposition approach is better than the one found in the full solution space, and the computational time is 38.5% shorter. The

key characteristic of the decomposed formulation that leads to shorter solution times for this example is the exclusion of integer variables from the control subproblem. In Table 10, one can see that although the control subproblem is almost as large as the complete direct formulation, its repetitive solution took only 64% of the 1154 CPUs of solution time for the whole decomposition algorithm. This is a much lower solution time per iteration than the 1876 CPUs for the direct formulation.

There are important differences between the MMA and the HIPS cases just presented. As problem size and complexity increase, the duality gap increases, but the benefits in terms of computational time become more significant. The same decomposition and solution methodology was used for the MMA case study and the HIPS case study, so the differences in performance can be attributed to a larger problem size (see Table 10) with stronger nonlinearities and nonconvexities in the HIPS case. Notice however, that the optimal found by using the decomposition technique is better for both examples.

Comparison of optimal solutions.

Table 9 shows that the overall transition time for the optimal solution found by the decomposition algorithm is less than that found by direct solution. Duration of transition times is key in obtaining a better hourly profit for the production cycle since they represent an unproductive period of the cycle. The cyclic scheduling model has the key feature of continuously depleting products so they are not kept until the end of the cycle. Therefore, the order of production does not influence inventory costs. Being this the case, the optimizer will always try to determine the sequence of production based on the shortest of transitions that in turn renders higher hourly profits. Figure 6 and 7 show the dynamic transitions of both solutions. The shapes of the transition profiles are similar, but the longest transition for the decomposition algorithm takes six hours vs. almost eight hours for the full space solution. The decomposition solution includes transitions between grades that are not adjacent in terms of MWD, like transitions A_2 to A_4 and

A_3 to Nm , as opposed to the sequence $Nm \rightarrow A_1 \rightarrow A_2 \rightarrow A_3 \rightarrow A_4$ chosen by the optimizer using the full solution space. The solution found by means of the decomposition heuristic avoids the need for a very long and expensive transition between the end of one cycle and the beginning of the next. This explains why the longest transition of the decomposed solution is two hours shorter than the longest transition of the direct solution.

The values of some decision variables for both solutions are found in Tables 11 and 12. A common characteristic of both solutions is that the quantity of grade A_3 produced is much greater than what is demanded. The cyclic scheduling formulation used in this work sets only a lower bound for production (demand must be satisfied) but sets no upper bound, since it assumes that all polymer produced is sold. Grade A_3 has the most favorable price to inventory costs proportion (raw material costs are the same for all grades), so it is easy to understand why most of the cycle is devoted to producing this grade, while all other grades are only produced to meet the demands. Also, the cycle resulting from the decomposed solution is shorter and more productive (total transition duration is shorter).

6.3 HIPS polymerization reaction train

The previous examples were solved using full solution space and using the described decomposition heuristic. The ultimate goal of the decomposition approach is not only to reduce computational effort and time, but to provide a solution for problems that are extremely difficult or even impossible to solve using the full space strategy. The following case study provides an example of a system where we could not obtain a solution using the full solution space.

Process Description

The system used for this case study is the High Impact Polystyrene free-radical bulk polymerization system. The mathematical model describing the process is shown in the

previous case example. In the present example the reaction is not carried out in a single CSTR but in a series of reactors²⁵. As displayed in Figure 9, the typical industrial set-up to carry out the HIPS polymerization reaction includes a CSTR, followed by a tubular reactor, and a heat exchanger were the reaction is completed. To represent the process without the complexities inherent in the modeling of tubular reactors, a mathematical model consisting of 7 CSTRs is used. The first reactor of the model represents the CSTR in the actual process; the following five CSTRs are used to model the tubular reactor, and the last CSTR in the model represents the heat exchanger. Each CSTR is modeled with a set of differential equations, equivalent to equations 39 - 45, 48, and 50. Table 13 shows the design parameters for the seven reactors of the model. The rest of the system parameters can be read from Table 7. Four different HIPS grades are produced, where each grade corresponds to a different steady state. Table 14 shows the values of the main processes variables and parameters that correspond to each steady state.

Results and Discussion

Figure 3 shows the evolution of the upper and lower bounding as the Lagrangean iterations proceed. This figure shows what Guignard²³ describes as a typical behavior of a “good” case when the subgradient method is being used for updating the Lagrange multipliers: a “sawtooth” pattern in the Lagrangean value for the first iterations, followed by a roughly monotonic improvement. The best lower bound, which corresponds to reported optimal solution, is found rather quickly, in less than 10 iterations. However, since the quality of the upper bound is improving considerably when this best lower bound is found, the algorithm is kept running. From iteration 30 onwards, the quality of the upper bound improves very slowly, while the lower bound keeps cycling among a few values. After 39 iterations the algorithm is stopped. At this point there is a 8.5% difference between upper and lower bounding. Once again, the best lower bound is reported as the best solution since all constraints of the original problem are satisfied, and therefore it is the

best feasible solution found by the algorithm. The optimal solution is reported in Table 15. Values of the most important decision variables for the optimal solution are found in Table 16. One of the key features of the solution is that the production wheel is carried out so that three grades (N, A, B) are produced to satisfy their demands (as required by the formulation) , and only grade C , which is the most profitable product, is produced over its demanded quantity (remember that there is no upper bound on production). Transition times are not compared against any other solution, but from previous analysis they are expected to be made as short as possible to achieve a productive manufacturing cycle.

Table 17 shows the size of the problem. In this example the most expensive subproblem is the control subproblem, in contrast to the heuristic subproblem, as in the previous examples. The extra complexity in the dynamic optimization of a train of reactors instead of just one CSTR is the main reason. Notice, once again, that the control subproblem does not include integer variables. The copy of the sequencing variables used in this subproblem is allowed to have continuous values between 0 and 1. The final value for the sequencing variables of the scheduling and the control subproblem for the last iteration of the decomposition algorithm are shown in Table 18. The same Table shows the values for the other duplicated variables for both subproblems. The values of the decision variables shown in this Table are not the optimal values found. The heuristic optimal solution is found in iteration number seven. Nevertheless, it is important to analyze the values of these variables in the last iteration in order to show how the algorithm deals with the duplicity of the variables copied in order to achieve the decomposition. The sequencing variables, y_{ik} for the scheduling subproblem are binary variables, while their copies in the control subproblem z_{ik} are allowed to have continuous values between 0 and 1. This fact is important since it is the key feature that reduces computational effort in the decomposition heuristic when compared against the direct solution. Notice that in the last iteration the values of both sets of variables are identical in some cases and almost the same for

others. In the worst cases the continuous variables have values of more than 0.99 or less than 0.01. This was achieved by the term in the objective function that penalizes the differences between copies of sequencing variables. Although the variables in the control subproblem are continuous they are forced by the algorithm to adopt values of exactly or very close to 0 and 1, so that the originally continuous variables behave very much like binary variables without the added complexity of this type of variables. Moreover, the sequence in the control subproblem is virtually the same as in the scheduling subproblem. The case is not the same for the transition durations and the cyclic time. Both subproblems still do not have the same values for the copied variables. These values might have eventually converged, but the time required for this convergence was considered not practical. Moreover, there is no mathematical guarantee that all duplicated variables will converge, even if the gap between upper and lower bound is minimized¹⁴. The objective of the algorithm of finding an optimal solution by heuristic lower bounding, while obtaining reasonable, well behaved upper bounds, is considered achieved after the determined number of iterations. This conclusion is validated by previous examples where a direct solution was available.

Dynamic behaviors of grade transitions in reactors 1,6 and 7 are shown in Figures 10-13. The profiles of these reactors correspond to the outlet of the actual process equipment: reactor 1 of the model is the actual CSTR, reactor 6 represents the last section of the actual tubular reactor, and reactor 7 of the model represents the process heat exchanger where the reaction is completed. Since the manipulated variable (monomer flow rate) is the same for the seven reactors at any given moment, there is only one dynamic profile per slot. The monomer flow rate during all grade transitions seems to follow the same pattern. The flow rate is decreased during the first part of the transition and then increased towards its steady state value. Such initial decrease in flow rate decreases the total cost of the transition since less monomer is wasted as off spec product. From Figures 10-13 one can see that in reactor one the controlled variables undergo small changes in

magnitude as they transition from one steady state to the next. This reactor has the lowest conversion values, so the operating temperatures are the lowest. In the initial stage the reaction rate is slower than in the rest of the reactors, and therefore the action of the manipulated variable does not have dramatic effects on the controlled variables. In contrast, the temperature and conversion inside reactor six, exhibit very fast responses to changes in the monomer flow rate. Recall that this reactor represents the last segment of the tubular reactor, which is modeled as a small CSTR. Since the volume is smaller than in the other two reactors (the residence time is shorter) and the temperatures are high, it is not surprising that the dynamic responses in this reactor are faster. Reactor 7 is similar in size to reactor 1, but its operating temperature is higher, so larger changes in conversion are carried out during grade transition. Duration of dynamic transitions in the HIPS reactor train is similar to dynamic transitions in the previous HIPS example, in which polymerization took place in only one CSTR. The longest transition for both examples takes around six hours. This means that the addition of a series of reactors instead of just one reactor should not result in a significant increase in transition costs in terms of wasted off spec material.

This last example illustrates how the decomposition heuristic described in this work represents a practical alternative for solving SSC problems, especially as they grow in size, nonlinearity and nonconvexity. In previous examples, although the computational effort of the decomposition approach was reduced, the solution in full space was available. However, in this last example it was impossible to find a solution in full space, using the same outer approximation algorithm (DICOPT) that was successfully used in previous examples. When trying to obtain a solution without the decomposition approach, the MINLP problem invariably became infeasible.

7 Conclusions

The Lagrangean Decomposition methodology as presented by Guignard and Kim¹ was used to reformulate the SSC problem^{10,4}. A solution methodology very similar to the one presented by Van den Heever et. al.² was used. According to this methodology the decomposed formulation is used to generate an upper bound and a heuristic procedure is used to generate a lower bound. The decomposition approach was successful for solving the SSC problem in the MMA example and in the HIPS polymerization system, using one CSTR and seven CSTRs. In the first two cases the optimal solution found by the decomposition approach was better than the solution obtained in the full space. Since both systems are highly nonlinear the better profit found by the decomposition approach is attributed to an increased number of local searches driven by the repetitive solution of the SSC problem in different iterations. In these two examples, the computational effort required by the decomposition heuristic is lower than the computational effort required by the direct solution (solution in full space). The third problem was only solvable using the decomposition heuristic. The present work does not prove that the solution to the SSC problem in the HIPS reactor train example cannot be obtained without the decomposition. However, it does show is that if such a direct solution is available, the effort required to obtain it becomes unpractical.

Future directions of our research include the simultaneous scheduling and control of even larger problems, as well as the simultaneous design, scheduling, and control of polymerization systems. The Lagrangean Decomposition Heuristic described in this paper could prove to be very useful in both cases.

Table 1: Design and Operation Parameters for the MMA Polymerization Reactors

$F = 1.0 \text{ m}^3/\text{h}$	$M_m = 100.12 \text{ kg}/\text{kgmol}$
$F_I = 0.0032 \text{ m}^3/\text{h}$	$f^* = 0.58$
$F_{cw} = 0.1588 \text{ m}^3/\text{h}$	$R = 8.314 \text{ kJ}/(\text{kgmol} \cdot \text{K})$
$C_{min} = 6.4678 \text{ kgmol}/\text{m}^3$	$-\Delta H = 57800 \text{ kJ}/\text{kgmol}$
$C_{Iin} = 8.0 \text{ kgmol}/\text{m}^3$	$E_p = 1.8283 \times 10^4 \text{ kJ}/\text{kgmol}$
$T_{in} = 350 \text{ K}$	$E_I = 1.2877 \times 10^5 \text{ kJ}/\text{kgmol}$
$T_{w0} = 293.2 \text{ K}$	$E_{fm} = 7.4478 \times 10^4 \text{ kJ}/\text{kgmol}$
$U = 720 \text{ kJ}/(\text{h} \cdot \text{K} \cdot \text{m}^2)$	$E_{tc} = 2.9442 \times 10^3 \text{ kJ}/\text{kgmol}$
$A = 2 \text{ m}^2$	$E_{td} = 2.9442 \times 10^3 \text{ kJ}/\text{kgmol}$
$V = 0.1 \text{ m}^3$	$A_p = 1.77 \times 10^9 \text{ m}^3/(\text{kgmol} \cdot \text{h})$
$V_0 = 0.02 \text{ m}^3$	$A_I = 3.792 \times 10^{18} \text{ 1}/\text{h}$
$\rho = 866 \text{ kg}/\text{m}^3$	$A_{fm} = 1.0067 \times 10^{15} \text{ m}^3/(\text{kgmol} \cdot \text{h})$
$\rho_w = 1000 \text{ kg}/\text{m}^3$	$A_{tc} = 3.8223 \times 10^{10} \text{ m}^3/(\text{kgmol} \cdot \text{h})$
$C_p = 2 \text{ kJ}/(\text{kg} \cdot \text{K})$	$A_{td} = 3.1457 \times 10^{11} \text{ m}^3/(\text{kgmol} \cdot \text{h})$
$C_{pw} = 4.2 \text{ kJ}/(\text{kg} \cdot \text{K})$	

Table 2: Steady States and grade information of the MMA polymerization reactor

	State A	State B	State C	State D	State E
$C_m \text{ (kmol}/\text{m}^3)$	5.5542	5.9653	6.0842	6.2341	6.3245
$T_{reactor} \text{ (K)}$	362	351	348	344	342
$X\%$	14	8	6	4	2
$MWD \text{ (kg}/\text{kmol})$	15000	25000	30000	39000	48000
$F_I \text{ (m}^3/\text{hr)}$	2.5×10^{-3}	3.2×10^{-3}	2.9×10^{-3}	2×10^{-3}	1.1×10^{-3}
Demand (kg/hr)	0.8	0.7	1	0.8	0.6
Inv. Cost (\$/hr-kg)	0.10	0.12	0.12	0.15	0.15
Mono. Cost (\$/lt _{feed})	10	10	10	10	10
Init. Cost (\$/lt _{feed})	500	500	500	500	500

Table 3: Direct and Lagrangean solutions for MMA example

Algorithm	Obj. [\$/hr]	Opt. Sequence	Cycle [hr]	Trans. [hr]	CPU [s]
Direct	81.6	$A \rightarrow B \rightarrow C \rightarrow D \rightarrow E$	149.4	14.9	128
Decomposed	83.6	$B \rightarrow A \rightarrow C \rightarrow E \rightarrow D$	139.9	14.0	107

Table 4: Problem Size for Direct and Decomposed Solution for MMA example. Percent of CPU time represents the time spent in each subproblem of the decomposed solution

Subproblem	Cont. variables	Discrete Variables	% CPU Time
MMA Direct	4927	25	
MMA Scheduling Subproblem	57	25	0.8
MMA Control Subproblem	4902	none	42
MMA Heuristic Subproblem	4927	none	57.2

Table 5: Simultaneous scheduling and control results in full space, for grade transition in a MMA polymerization CSTR. The objective function value is \$ 81.6/hr and 149 h of total cycle time.

Product	Process T [h]	production [kg]	Trans T [h]	T start[h]	T end [h]
<i>A</i>	29.88	119.51	2.83	0	32.70
<i>B</i>	20.91	104.57	1.60	62.19	55.22
<i>C</i>	37.35	149.39	1.99	101.24	94.56
<i>D</i>	23.90	119.51	1.69	127.57	120.15
<i>E</i>	22.41	89.63	6.83	127.57	149.39

Table 6: Simultaneous scheduling and control results using decomposition heuristic, for grade transition in a MMA polymerization CSTR. The objective function value is \$ 83.6/hr and 140 h of total cycle time.

Product	Process T [h]	production [kg]	Trans T [h]	T start[h]	T end [h]
<i>B</i>	19.58	97.89	3.22	0	22.80
<i>A</i>	27.97	111.88	3.18	22.80	53.95
<i>C</i>	34.96	139.85	2.76	53.95	91.67
<i>E</i>	20.98	83.91	1.52	91.67	114.17
<i>D</i>	22.38	111.88	3.30	114.17	139.85

Table 7: Nominal parameter values for an industrial scale HIPS CSTR.

Parameter	Value	Units	Parameter	Value	Units
Q	1.1411813934	L/s	T_j^f	294	K
C_i^f	0.9814814815	mol/L	T^f	333	K
Q_i	0.0015	L/s	Q_w	1	L/s
C_m^f	8.6310347459	mol/L	C_b^f	1.0547874055	mol/L
V	9450	L	V_c	2000	L
f^*	0.57		ΔH_r	69919.56	J/mol
ρ_s	0.915	kg/L	C_{ps}	1647.265	J/(kg-K)
ρ_w	1	kg/L	C_{pw}	4045.7048	J/(kg-k)
A	19.5	m ²	U	80	J/(s-K-m ²)
R	1.9858	cal/(mol-K)	A_{i0}	1.1x10 ⁵	L ² /(mol ² -s)
E_{i0}	27340	cal/mol	A_d	9.1x10 ¹³	1/s
E_d	29508	cal/mol	A_{i1}	1x10 ⁷	L/(mol-s)
E_{i1}	7067	cal/mol	A_{i2}	2x10 ⁶	L/(mol-s)
E_{i2}	7067	cal/mol	A_{i3}	1x10 ⁷	L/(mol-s)
E_{i3}	7067	cal/mol	A_p	1x10 ⁷	L/(mol-s)
E_p	7067	cal/mol	A_t	1.7x10 ⁹	L/(mol-s)
E_t	843	K	A_{fs}	6.6x10 ⁷	L/(mol-s)
E_{fs}	14400	cal/mol	A_{fb}	2.3x10 ⁹	L/(mol-s)
E_{fb}	18000	cal/mol			

Table 8: Steady States and grade information of the HIPS polymerization reactor

	State Nm	State A1	State A2	State A3	State A4
C_m	6.0725	6.6229	6.0842	8.5536	8.600
$T_{reactor}$	389	381	348	330	320
$X\%$	30	23	10	1	0.5
MWD	118000	125000	148000	343000	489000
Q_w [L/s]	1.0	0.5	0.1	0.1	0.5
Demand [kg/hr]	50	60	65	70	60
Price [\$/kg]	3.2	4.3	4.5	5.0	5.5
Inv. Cost [\$/hr-kg]	0.15	0.20	0.15	0.10	0.25
Mono. Cost [\$/lt _{feed}]	1	1	1	1	1
Init. Cost [\$/lt _{feed}]	10	10	10	10	10

Table 9: Direct and Lagrangian solutions for HIPS example

Algorithm	Obj. [\$/hr]	Opt. Sequence	Cycle [hr]	Trans. [hr]	CPU [s]
Direct	10500.1	$Nm \rightarrow A_1 \rightarrow A_2 \rightarrow A_3 \rightarrow A_4$	88.4	12.6	1876
Decomposed	10568.2	$A_2 \rightarrow A_4 \rightarrow A_3 \rightarrow N_m \rightarrow A_1$	87.1	12.2	1154

Table 10: Problem Size for Direct and Decomposed Solution for HIPS example. Percent of CPU time represents the time spent in each subproblem of the decomposed solution

Subproblem	Cont. variables	Discrete Variables	% CPU Time
HIPS Direct	13452	25	
HIPS Scheduling Subproblem	62	25	0.07
HIPS Control Subproblem	13422	none	35.62
HIPS Heuristic Subproblem	13452	none	64.31

Table 11: Simultaneous scheduling and control results in full space, for grade transition in a HIPS polymerization CSTR. The objective function value is \$ 10500/hr and 88.4 h of total cycle time.

Product	Process T [h]	production [kg]	Trans T [h]	T start[h]	T end [h]
Nm	2.00	4421.3	0.98	0	2.18
A_1	1.44	5305.6	1.80	2.18	5.42
A_2	1.56	5747.8	1.65	5.42	8.63
A_3	70.18	2.5915e5	0.50	8.63	79.30
A_4	1.44	5305.6	7.69	79.30	88.43

Table 12: Simultaneous scheduling and control results using decomposition heuristic, for grade transition in a HIPS polymerization CSTR. The objective function value is \$ 10568/hr and 87.1 hrs of total cycle time.

Product	Process T [h]	production [kg]	Trans T [h]	T start[h]	T end [h]
A_2	1.53	5659.87	2.02	0	3.55
A_4	1.42	5659.87	1.39	3.55	6.35
A_3	69.34	2.5607e5	6.01	6.35	81.70
Nm	1.18	4353.75	0.98	81.70	83.86
A_1	1.42	5224.59	1.80	83.86	87.08

Table 13: Design parameters for the seven reactors of the HIPS reaction train. Q_{cw} stands for cooling water flow rate.

Reactor	Volume [L]	Jacket Volume [L]	Q_{cw} [L/s]	Heat-Transfer Area [m^2]
1	6000	1200	0.1311	11.718
2	900	180	1.0	1.7578
3	1000	200	1.0	1.9531
4	650	130	1.0	1.2695
5	1000	200	1.0	1.9531
6	1000	200	1.0	1.9531
7	5000	1000	1.0	9.5676

Table 14: Steady States and grade information of the HIPS polymerization reaction train. State values and conversion correspond the last CSTR of the reaction train.

	State N	State A	State B	State C
C_m [mol/L]	3.1344	2.3018	1.4534	0.7519
$T_{Reactor}$ [K]	395	440	476	517
$X\%$	64	73	83	91
Q_m [L/s]	1.14	1.48	1.64	2.10
Demand [kg/hr]	350	325	300	250
Price [\$/kg]	3.2	4.3	4.5	5.0
Inv. Cost [\$/hr-kg]	0.16	0.21	0.22	0.25
Mono. Cost [\$/lt _{feed}]	1	1	1	1
Init. Cost [\$/lt _{feed}]	100	100	100	100

Table 15: Lagrangean solution for HIPS train example

Algorithm	Obj. [\$/hr]	Opt. Sequence	Cycle [hr]	Trans. [hr]	CPU [s]
Decomposed	6244.5	$A \rightarrow N \rightarrow C \rightarrow B$	39.2	12.2	10600

Table 16: Simultaneous scheduling and control results using decomposition heuristic, for grade transition in a HIPS polymerization train. The objective function value is \$ 6245/hr and 39.2 hrs of total cycle time.

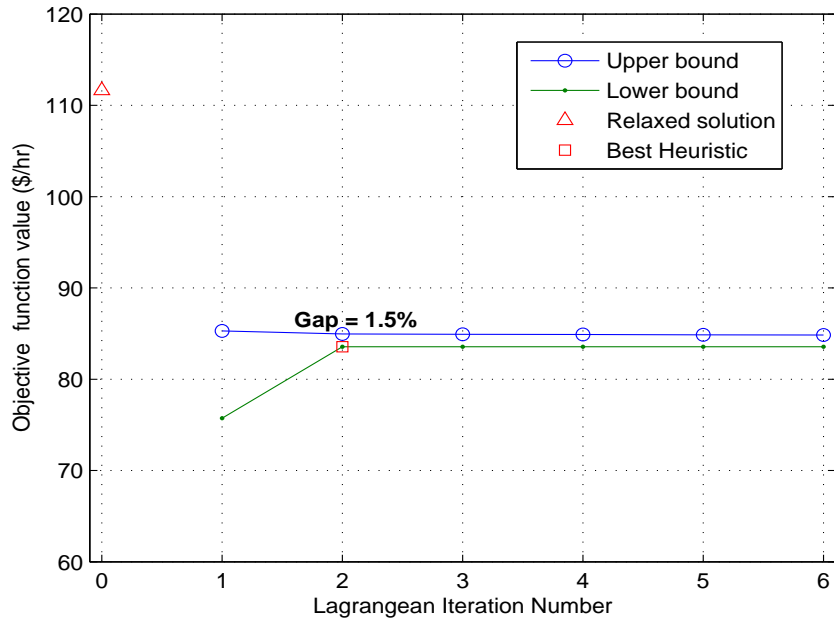
Product	Process T [h]	production [kg]	Trans T [h]	T start[h]	T end [h]
A	3.72	12742.20	5.96	0	8.62
N	2.66	13722.37	3.37	8.62	15.72
C	18.40	1.2501e5	1.43	15.72	35.54
B	2.22	11762.03	1.45	35.54	39.21

Table 17: Problem Size for Direct and Decomposed Solution for HIPS train example. Percent of CPU time represents the time spent in each subproblem of the decomposed solution

Subproblem	Cont. variables	Discrete Variables	% CPU Time
HIPS Scheduling Subproblem	46	16	0.03
HIPS Control Subproblem	22678	none	67.76
HIPS Heuristic Subproblem	22702	none	32.21

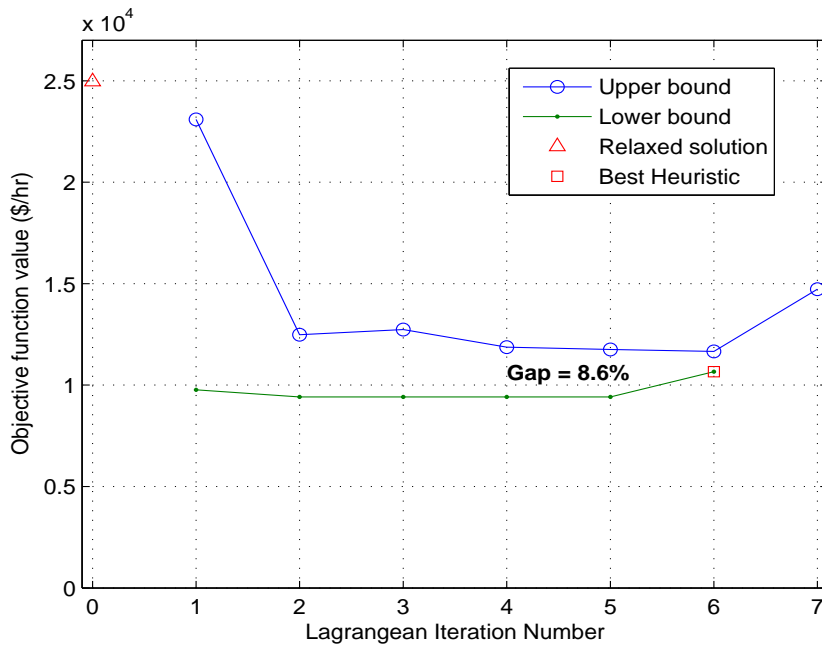
Table 18: Value of the duplicated variables in the last Lagrangean iteration. The best upper bound is found in this last iteration, corresponding to an objective value of \$ 6823.58 /hr. Binary variables, and their continuous equivalents in the control subproblem, not shown have a value of 0.

Variable	Scheduling Subproblem	Control Subproblem
y_{B1}	1	-
y_{A2}	1	-
y_{N3}	1	-
y_{C4}	1	-
z_{B1}	-	0.994
z_{A2}	-	0.994
z_{N3}	-	1.000
z_{C4}	-	1.000
z_{A1}	-	0.006
z_{B2}	-	0.006
θ_1^t	0.50	-
θ_2^t	0.50	-
θ_3^t	0.50	-
θ_4^t	0.50	-
ϕ_1^t	-	1.43
ϕ_2^t	-	6.60
ϕ_3^t	-	3.31
ϕ_4^t	-	1.43
Tc	16.634	-
Dc	443.486	-



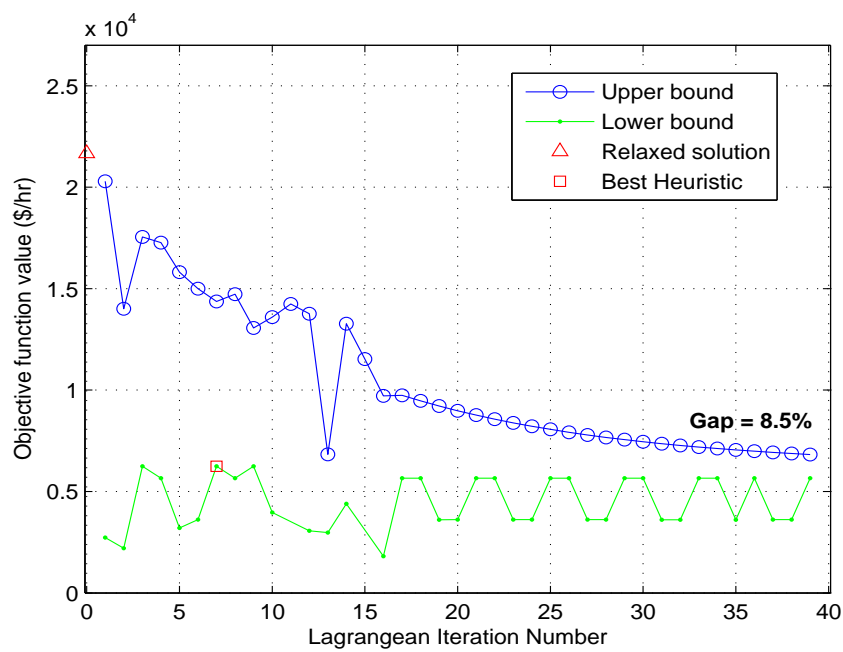
[c]

Figure 1: Upper and lower bounds evolution during Lagrangean Heuristic for MMA example.



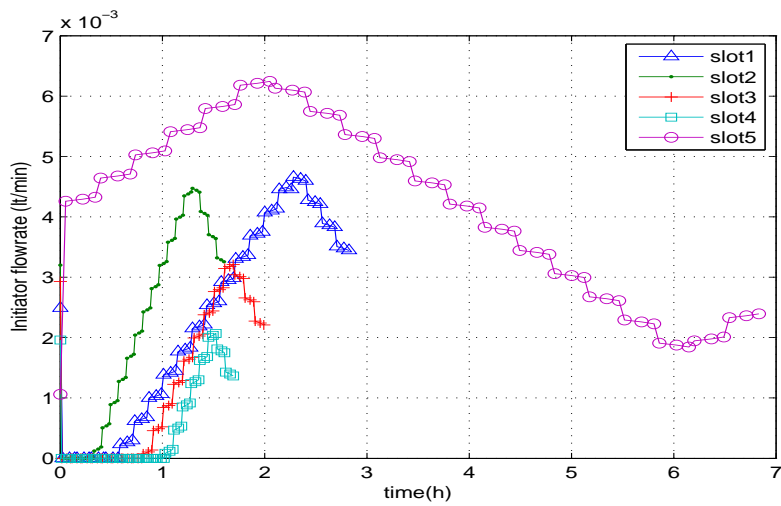
[[c]

Figure 2: Upper and lower bounds evolution during Lagrangean Heuristic for HIPS example.

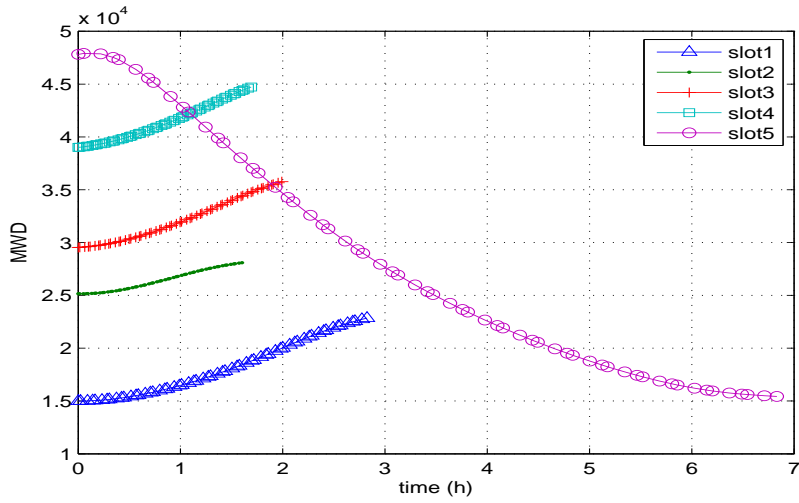


[c]

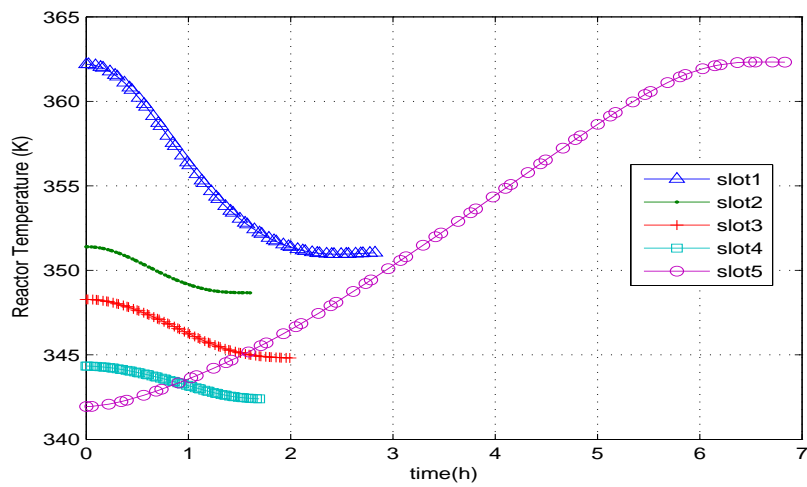
Figure 3: Upper and lower bounds evolution during Lagrangean Heuristic for HIPS example.



(a)

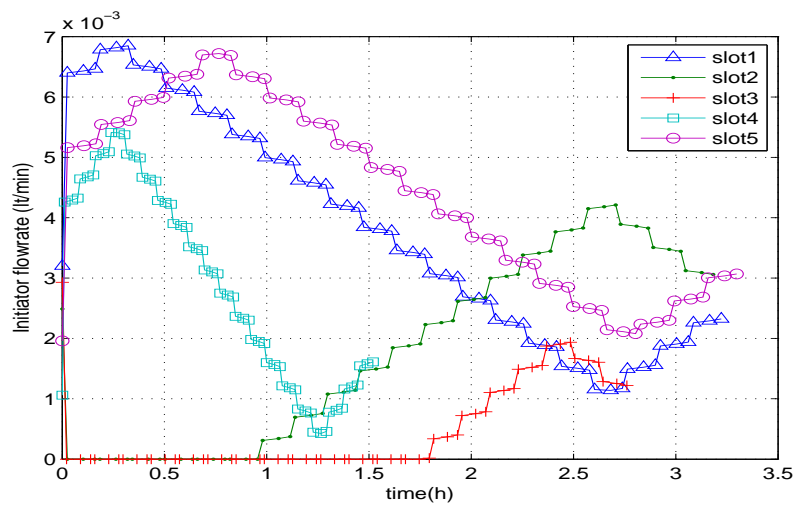


(b)

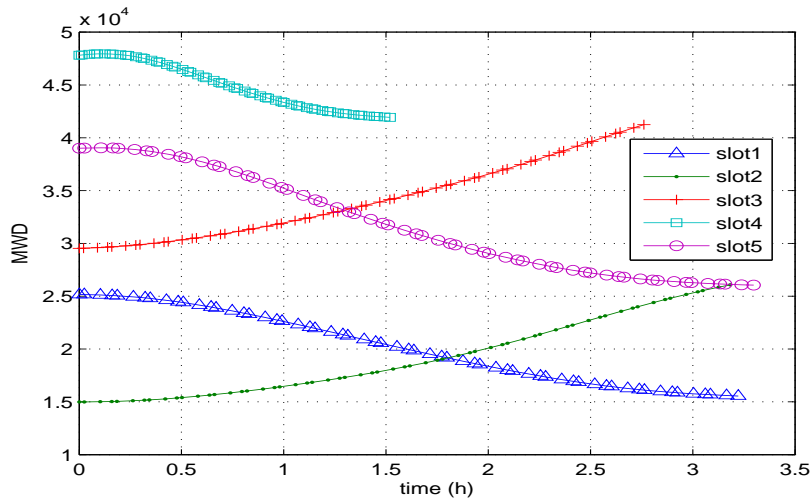


(c)

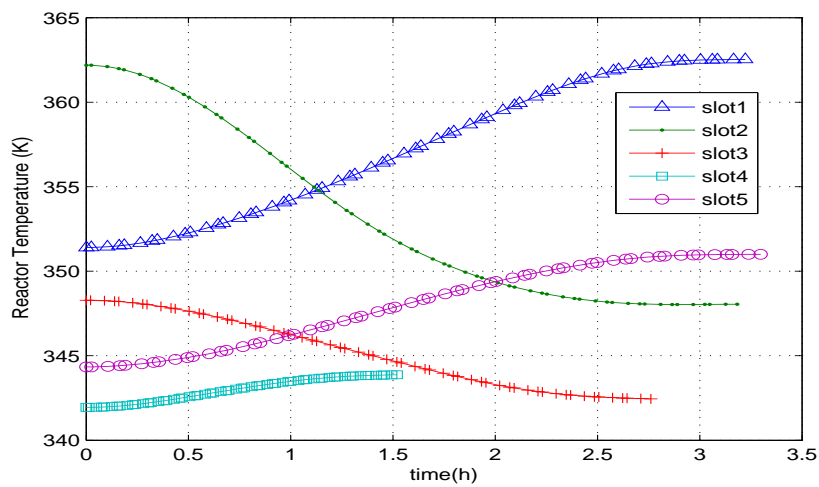
Figure 4: Dynamic transitions for the MMA example obtained by direct solution: (a) Manipulated variable (b) MWD (c) Reactor Temperature



(a)

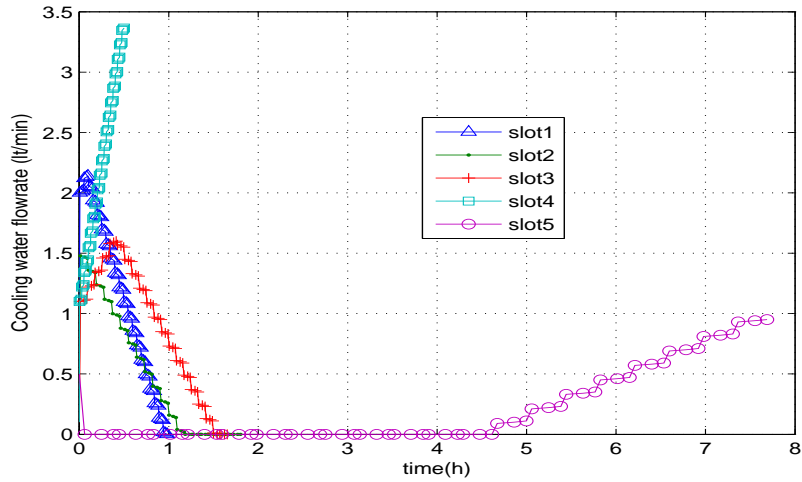


(b)

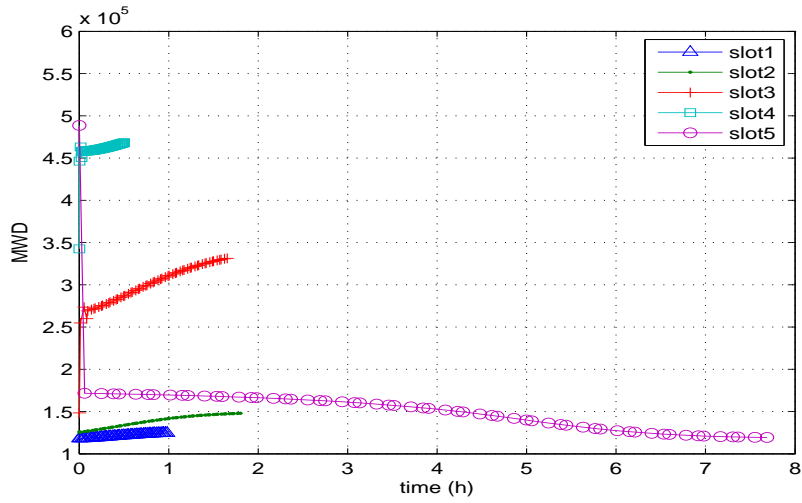


(c)

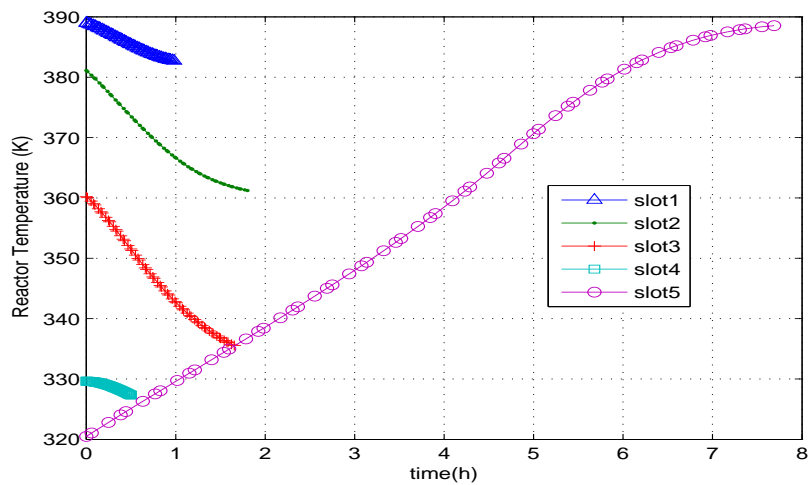
Figure 5: Dynamic transitions for the MMA example obtained by Lagrange Heuristic: (a) Manipulated variable (b) MWD (c) Reactor Temperature



(a)

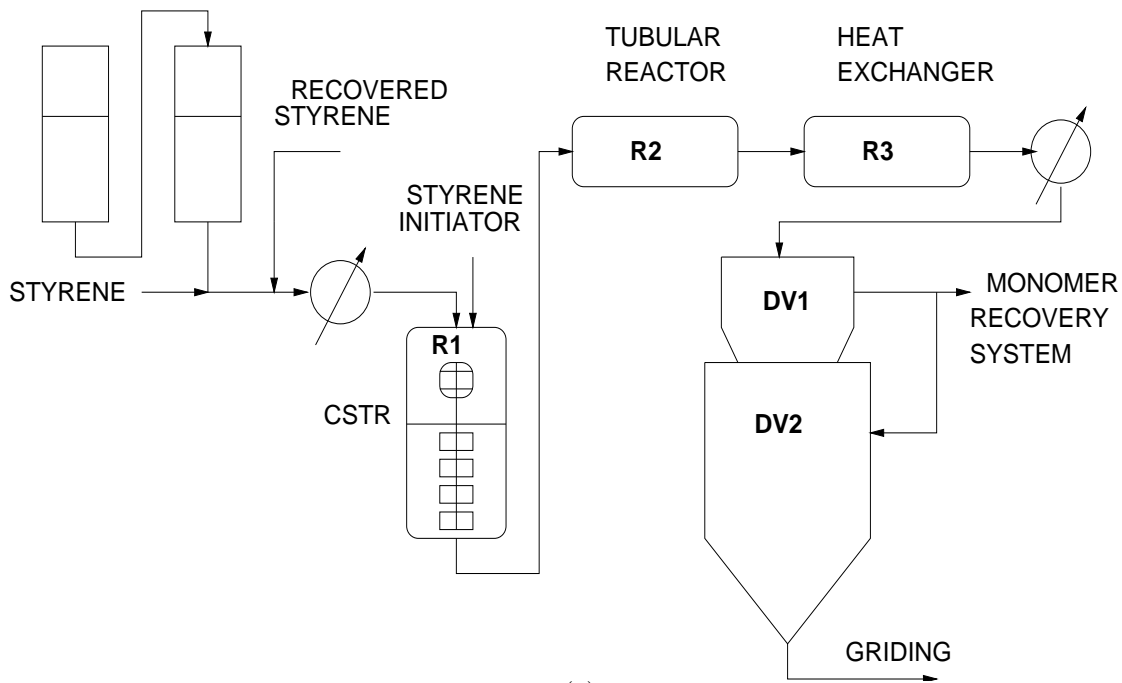


(b)

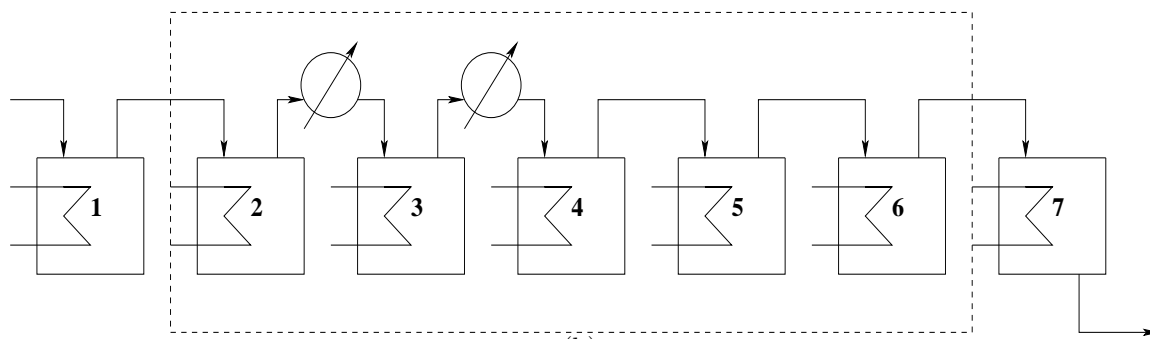


(c)

Figure 6: Dynamic transitions for the HIPS example obtained by direct solution: (a) Manipulated variable (b) MWD (c) Reactor Temperature



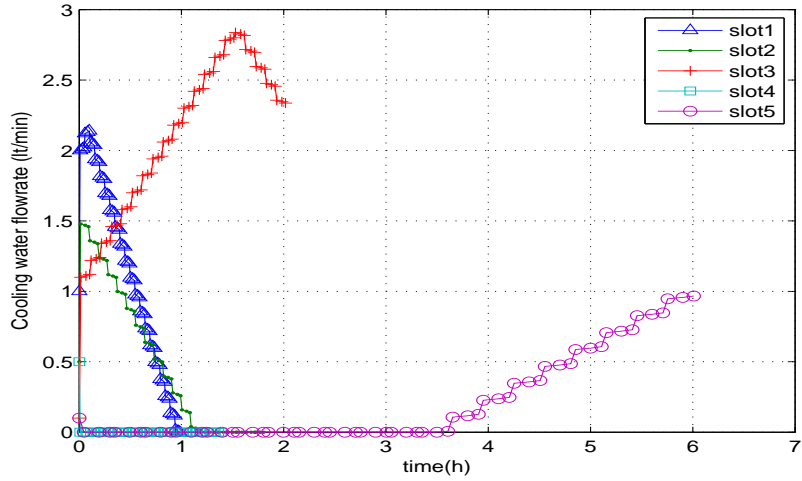
(a)



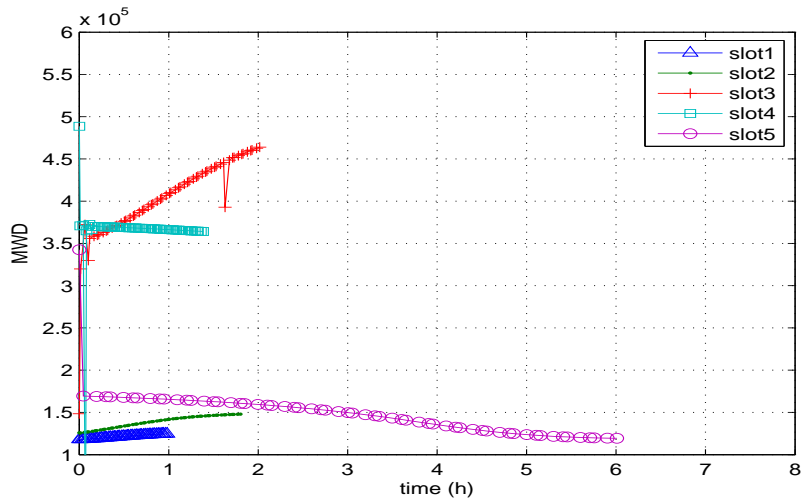
(b)

Figure 8:

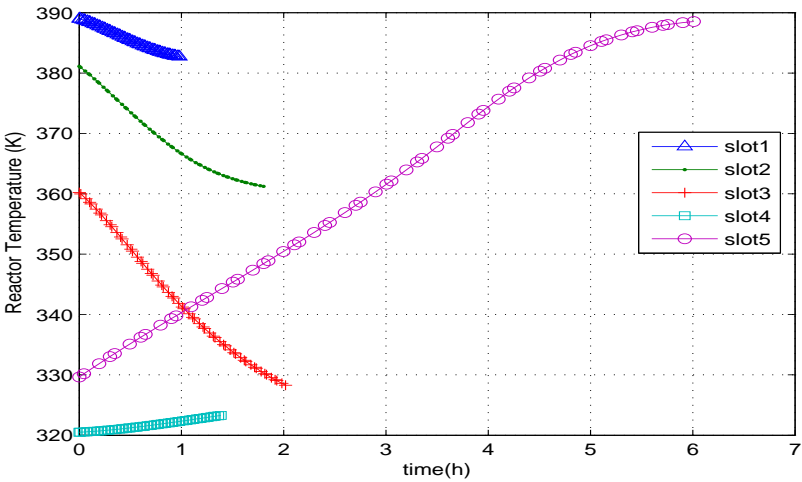
Figure 9: (a) Flowsheet of the HIPS plant, (b) Approximation of the HIPS plant by a set of 7 series-connected CSTRs. The dashed box stands for the 5 CSTRs employed for approximating the steady-state behavior of the R2 tubular reactor.



(a)

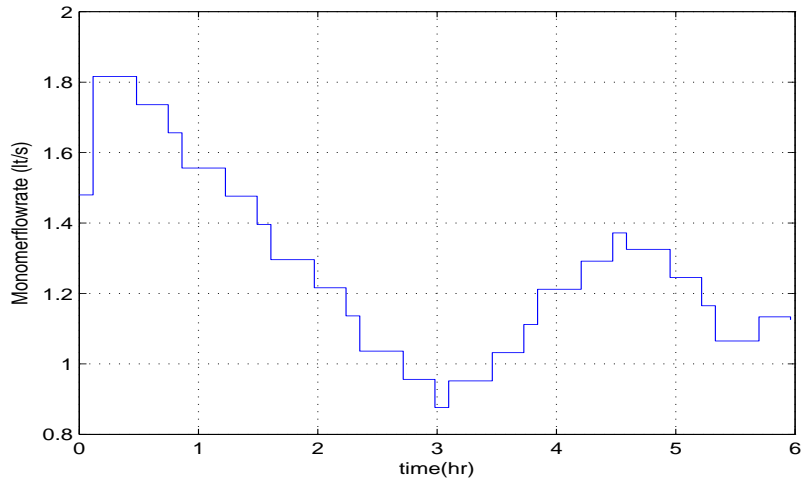


(b)

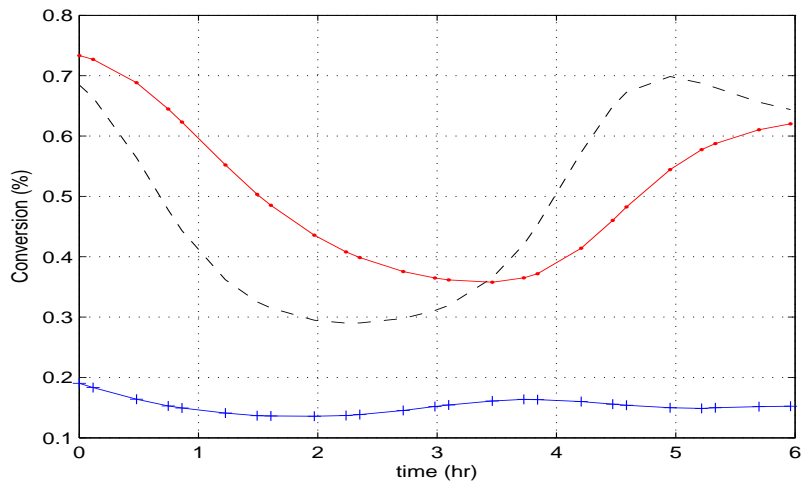


(c)

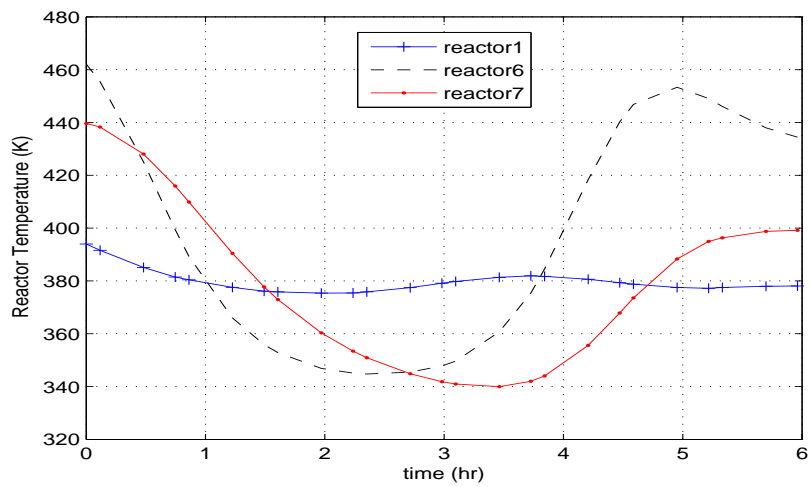
Figure 7: Dynamic transitions for the HIPS example obtained by Lagrange Heuristic solution: (a) Manipulated variable (b) MWD (c) Reactor Temperature



(a)

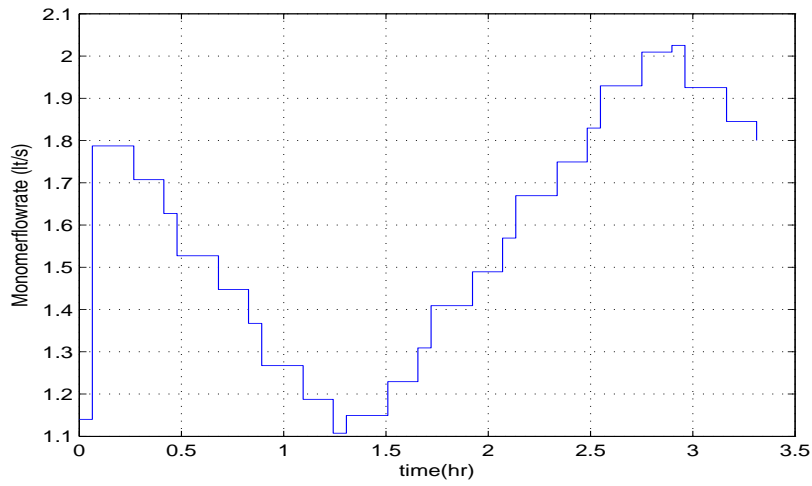


(b)

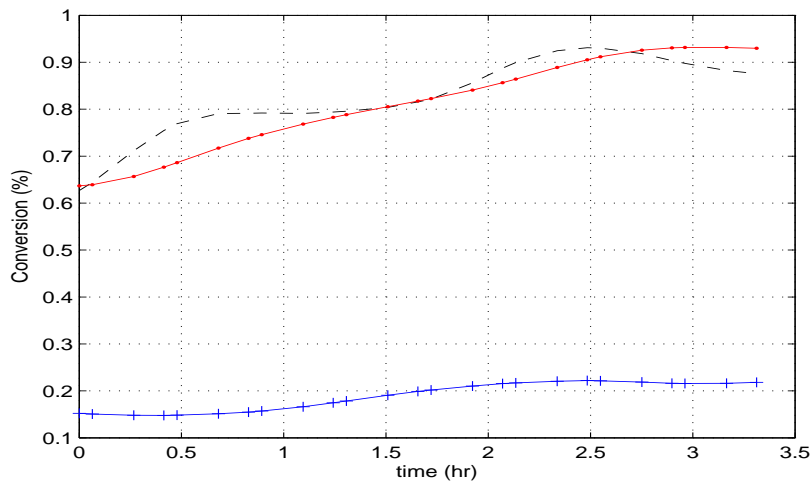


(c)

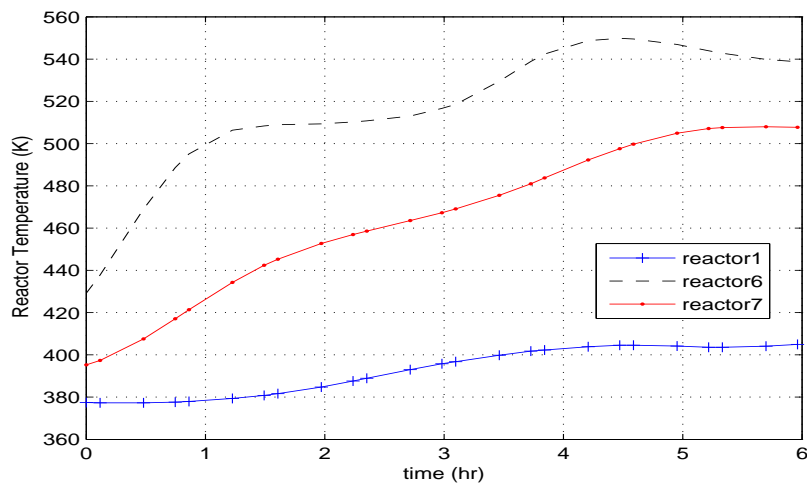
Figure 10: Monomer feed stream (a) conversion (b) and temperature profiles (c) of reactors 1,6 and 7 in slot 1.



(a)

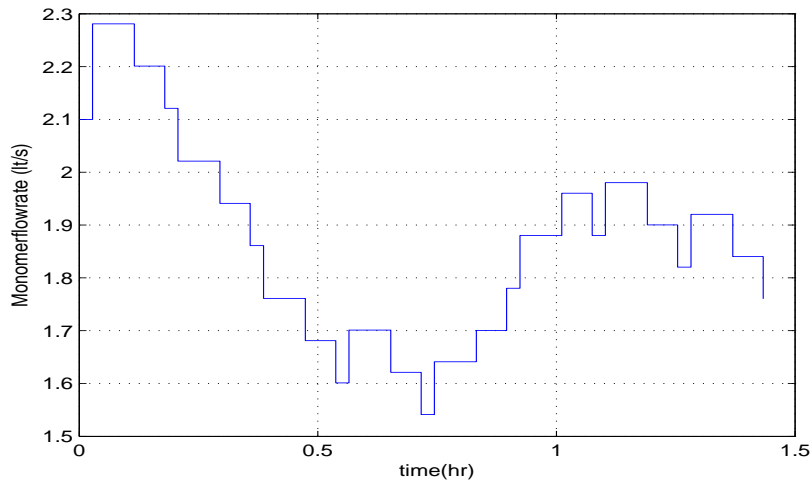


(b)

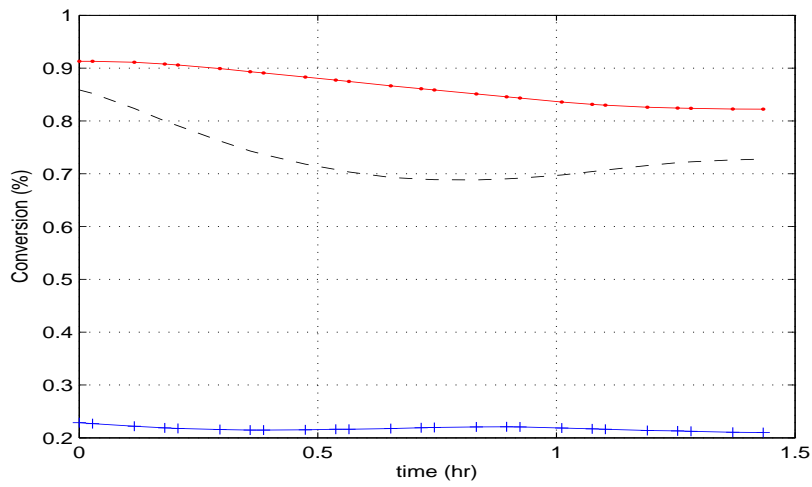


(c)

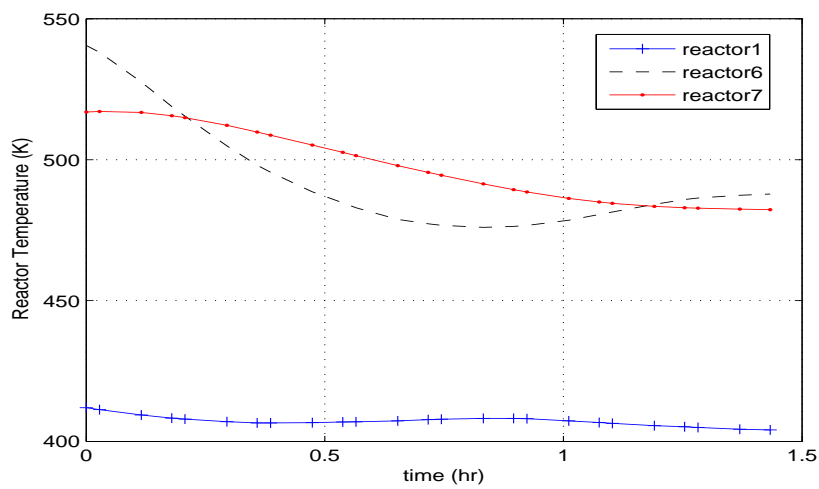
Figure 11: Monomer feed stream (a) conversion (b) and temperature profiles (c) of reactors 1,6 and 7 in slot 2.



(a)



(b)



(c)

Figure 12: Monomer feed stream (a) conversion (b) and temperature profiles (c) of reactors 1,6 and 7 in slot 3.

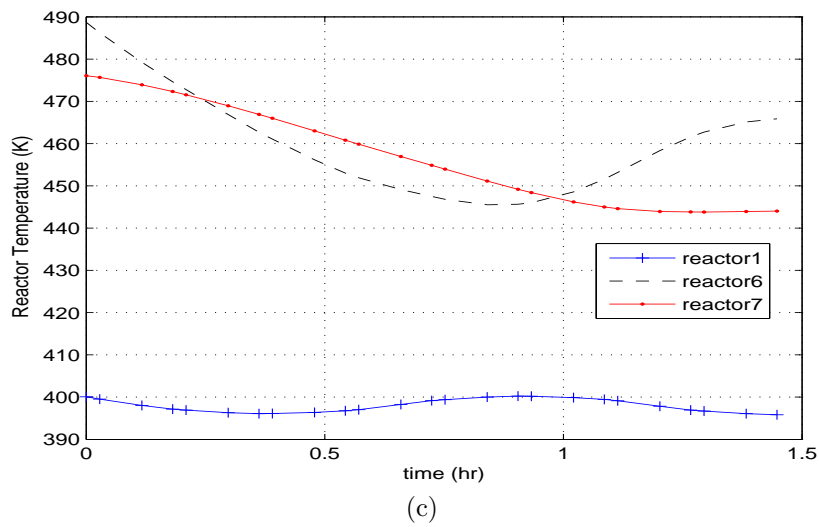
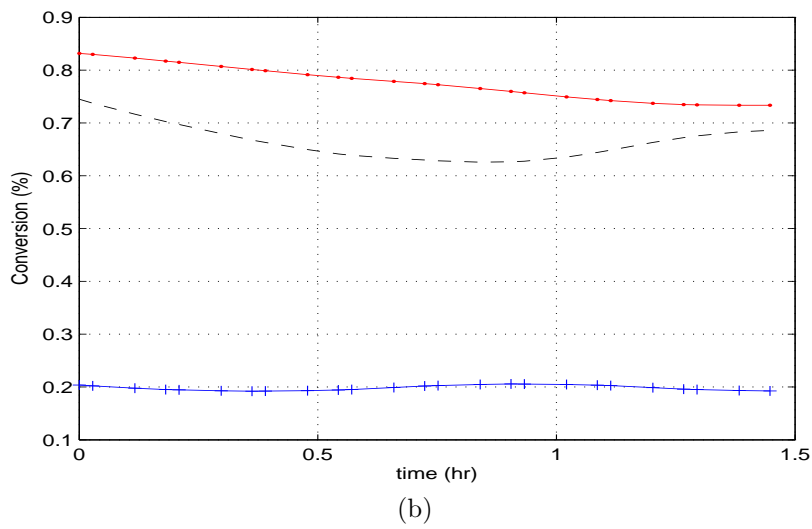
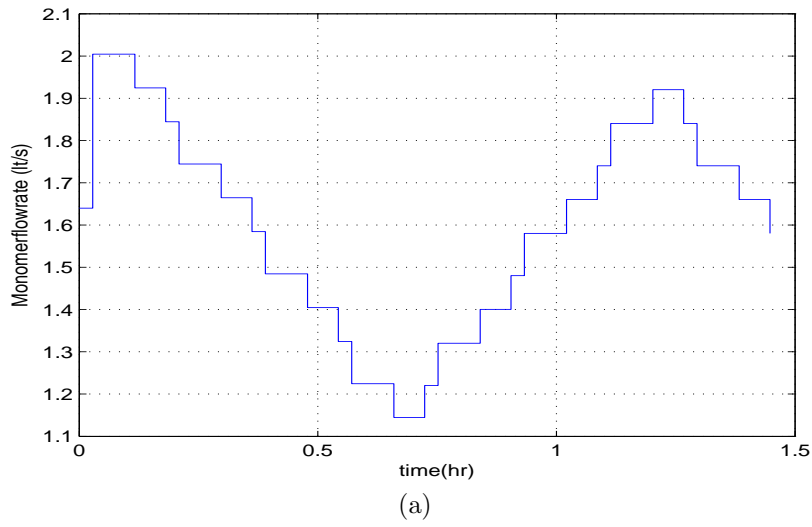


Figure 13: Monomer feed stream (a) conversion (b) and temperature profiles (c) of reactors 1,6 and 7 in slot 4.

References

- [1] Guignard M., Kim S.. Lagrangean Decomposition: A model yielding Stronger Lagrangean Bounds *Mathematical Programming.* 1987;39:215-228.
- [2] Van-Heerden S.A., Grossmann I.E., Vasantharajan S., Edwards K.. A Lagrangean Decomposition Heuristic for the Design and Planning of Offshore Hydrocarbon Field Infrastructures with Complex Economic Objectives *Ind. Eng. Chem. Res.* 2001;40:2857-2875.
- [3] Mishra B.V., Mayer E., Raisch J., Kienle A.. Short-Term Scheduling of Batch Processes. A Comparative Study of Different Approaches *Ind. Eng. Chem. Res.* 2005;44:4022-4034.
- [4] Terrazas-Moreno S., Flores-Tlacuahuac A., Grossmann I.E.. Simultaneous Cyclic Scheduling and Optimal Control of Polymerization Reactors *Submitted for revision.* 2006.
- [5] Mahadevan R., Doyle F.J. III, Allcock A.C.. Control-Relevant Scheduling of Polymer Grade Transitions *AICHE J.* 2002;48(8):1754-1764.
- [6] Feather D., Harrell D., Liberman R., Doyle F.J.. Hybrid Approach to Polymer Grade Transition Control *AICHE J.* 2004;50(10):2502-2513.
- [7] Prata A., Oldenburg J., Marquardt W., R. Nystrom A. Kroll. Integrated Scheduling and Dynamic Optimization of Grade Transitions for a Continuous Polymerization Reactor *Submitted for revision.* .
- [8] Nystrom R.H., Franke R., I.Harjunkoski , A.Kroll . Production Campaign Planning including Grade Transition Sequencing and Dynamic Optimization *Comput. Chem. Eng.* 2005;29(10):2163-2179.
- [9] Nystrom R.H., I.Harjunkoski , A.Kroll . Production Optimization for continuously

- operated processes with optimal operation and scheduling of multiple units *Comput. Chem. Eng.*. 2006;30:392-406.
- [10] Flores-Tlacuahuac A., Grossmann I.E.. Simultaneous Cyclic Scheduling and Control of a Multiproduct CSTR *Ind. Eng. Chem. Res.*. 2006;45(20):6698-6712.
- [11] Biegler L.T.. Optimization strategies for complex process models *Advances in Chemical Engineering*. 1992;18:197-256.
- [12] deMatta R.. A Lagrangean decomposition solution to a single line multiproduct scheduling problem *European Journal of Operational Research*. 1994;79:25-37.
- [13] Wu D., Ierapetritou M.G.. Decomposition approaches for the efficient solution of short-term scheduling problems *Comput. Chem. Eng.*. 2003;27:1261-1276.
- [14] Wu D., Ierapetritou M.. Lagrangean decomposition using an improved Nelder-Mead approach for Lagrangean multiplier update *Comput. Chem. Eng.*. 2003;27:1261-1276.
- [15] Finlayson B.. *Nonlinear Analysis in Chemical Engineering*. New York: McGraw-Hill 1980.
- [16] Villadsen , J. , M.Michelsen . *Solution of Differential Equations Models by Polynomial Approximation*. Prentice-Hall 1978.
- [17] Fisher M.L. The Lagrangean Relaxation Method for Solving Integer Programming Problems *Management Science*. 1981;27(1):1.
- [18] Guignard M.. Lagrangean Relaxation: A Short Course *Belg. J. OR.: Special Issue Francoro*. 1995;35:3.
- [19] Geoffrion A.M.. Lagrangean Relaxation for Integer Programming *Math. Program. Study 2*. 1974;2:82-114.
- [20] Fisher M.L.. An Application Oriented Guide to Lagrangian Relaxation *Interfaces*. 1985;15(2):10.

- [21] Michelon P., Maculan N.. Lagrangean Decomposition for Integer Nonlinear Programming with Linear Constraints *Mathematical Programming.* 1991;52:203-313.
- [22] Silva-Beard S., Flores-Tlacuahuac A.. Effects of Process Design/Operation on the Steady-State Operability of a Methyl-Methacrylate Polymerization Reactor *Ind. Eng. Chem. Res.* 1999;38:4790-4804.
- [23] Guignard M.. Lagrangean Relaxation *Top.* 2003;11(2):151-228.
- [24] Flores-Tlacuahuac A., Verazaluce-García J.C., Saldívar-Guerra E.. Steady-State Nonlinear Bifurcation Analysis of a High Impact Polystyrene Continuous Stirred Reactor *Ind. Eng. Chem. Res.* 2000;39:1972-1979.
- [25] Flores-Tlacuahuac A., Biegler L.T., Saldívar-Guerra E.. Dynamic Optimization of HIPS Open-Loop Unstable Polymerization Reactors *Ind. Eng. Chem. Res.* 2005;44:2659-2674.

Appendix

The indices, decision variables and system parameters used in the SSC MIDO problem formulation are as follows:

1. Indices

Products	$i, p = 1, \dots, N_p$
Slots	$k = 1, \dots, N_s$
Finite elements	$f = 1, \dots, N_{fe}$
Collocation points	$c, l = 1, \dots, N_{cp}$
System states	$n = 1, \dots, N_x$
Manipulated variables	$m = 1, \dots, N_u$

2. Decision variables

y_{ik}	Binary variable to denote if product i is assigned to slot k
z_{ik}	Copy of y_{ik}
p_k	Processing time at slot k
t_k^e	Final time at slot k
t_k^s	Start time at slot k
t_{fck}	Time at finite element f and collocation point c of slot k
G_i	Production rate
Tc	Cyclic time [h]
Dc	Copy of Tc
x_{fck}^n	n -th system state in finite element f and collocation point c of slot k
\dot{x}_{flk}^n	Value of n -th state derivative with respect to time in finite element f and collocation point l of slot k
u_{fck}^m	m -th manipulated variable in finite element f and collocation point c of slot k

W_i	Amount produced of each product [kg]
θ_{ik}	Processing time of product i in slot k
θ_k^t	Transition time at slot k
ϕ_k^t	Copy of θ_k^t
Θ_i	Total processing time of product i
$x_{o,fk}^n$	n -th state value at the beginning of the finite element f of slot k
\bar{x}_k^n	Desired value of the n -th state at the end of dynamic transition of slot k
\bar{u}_k^m	Desired value of the m -th manipulated variable at the end of dynamic transition of slot k
$x_{in,k}^n$	n -th state value at the beginning of dynamic transition of slot k
$u_{in,k}^m$	m -th manipulated variable value at the beginning of dynamic transition of slot k
X_{fck}	Conversion in finite element f and collocation point c of slot k
MWD_{fck}	Molecular Weight Distribution in finite element f and collocation point c of slot k

3. Parameters

N_p	Number of products
N_s	Number of slots
N_{fe}	Number of finite elements
N_{cp}	Number of collocation points
N_x	Number of system states
N_u	Number of manipulated variables

D_i	Demand rate [kg/h]
C_i^p	Price of products [\$/kg]
C_i^s	Cost of inventory [\$/kg-hr]
C^r	Cost of raw material [\$/lt of feed solution]
C^I	Cost of initiator [\$/lt of feed solution]
h_{fk}	Length of finite element f in slot k
Ω_{cc}	Matrix of Radau quadrature weights
\bar{x}_k^n	Desired value of the n -th system state at slot k
\bar{u}_k^m	Desired value of the m -th manipulated variable at slot k
θ^{max}	Upper bound on processing time
$x_{ss,i}^n$	n -th state value at steady state of product i
$u_{ss,i}^m$	m -th manipulated variable value of product i
F_i^o	Feed stream volumetric flow rate at steady state for grade i
$MW_{monomer}$	Monomer molecular weight [kg/kmol]
$X_{ss,i}$	Desired conversion degree of grade i
$MWD_{ss,i}$	Desired molecular weight distribution of grade i
x_{min}^n, x_{max}^n	Minimum and maximum value of the state x^n
u_{min}^m, u_{max}^m	Minimum and maximum value of the manipulated variable u^m
\dot{x}_{tol}^n	Maximum absolute value for state derivatives at the end of dynamic transition
x_{tol}^n	Maximum absolute deviation from desired final value, allowable for state variable x^n at the end of dynamic transition
u_{cont}^f	Maximum absolute change for u^m between finite elements
u_{cont}^c	Maximum absolute change for u^m between collocation points
γ_c	Roots of the Lagrange orthogonal polynomial
Q_{max}^m	Maximum monomer flow rate [lt/hr]
Q_{max}^I	Maximum initiator flow rate [lt/hr]